Characterisation of ashes from waste biomass power plants and phosphorus recovery

Lijian Leng [a], Anna A. Bogush [b], Amitava Roy [c], Julia A. Stegemann [b *]

[a] *School of Resources, Environmental & Chemical Engineering and Key Laboratory of Poyang Lake Environment and Resource Utilization, Ministry of Education, Nanchang University, Nanchang, 330031, China*

[b] *Centre for Resource Efficiency & the Environment, Department of Civil, Environmental & Geomatic Engineering, University College London, Chadwick Building, Gower Street, London WC1E 6BT, UK*

[c] *J. Bennett Johnston, Sr., Center for Advanced Microstructures & Devices, Louisiana State University, 6980 Jefferson Hwy, Baton Rouge, LA 70806, USA*

[*] *Corresponding author. Tel.: +44 (0)2076797370*

E-mail address: j.stegemann@ucl.ac.uk (J.A. Stegemann)

Response to reviewers' comments

Reviewer #1:

Manuscript Number: STOTEN-D-19-07294

Characterisation of ashes from waste biomass power plants and phosphorus recovery.

The manuscript is dealing with a very interesting and important topic related to using of ashes as P nutrient. It is still quite few papers written on the topic on characterization and P recovery, and more knowledge is needed. The overall impression is that the manuscript is well organized and written. The title is adequate and covers the content of the manuscript. The objectives are well defined and the tables and the figure are well formed and arranged. The result and discussion is very comprehensive and in depth discussed. The literature referred to is relevant and show that the authors have good overview of what is published on the topic. Some written papers on phosphorus in waste products not refereed to could however give important input to the paper. The results are worth to be published.

Response: We appreciate the reviewer's positive comments.

I have only a very few comments to this manuscript:

Line 103-108: A comprehensive work on characterization of ashes, meat/bone meal and manures has been done by Brod et al. (2015) and should be referred to as work done on ashes.

Brod, E., Øgaard, A.F., Hansen, E., Wragg, D., Haraldsen, T.K. & Krogstad, T. (2015). Waste products as alternative phosphorus fertilisers. Part I: Characterised inorganic P species affect fertilization effects dependent on soil pH. Nutr Cycl Agroecosyst. 103 (2):167-185.

Brod, E., Øgaard, A.F., Haraldsen, T.K. & Krogstad, T. (2015). Waste products as alternative phosphorus fertilisers. Part II: Predicting P fertilization effects by chemical extraction. Nutr Cycl Agroecosyst. 103 (2):187-199.

Line 242: In addition to Rajendran et al. (2013) a reference to Brod et al. (2015) can be added.

Response: We have included the references mentioned by the reviewer to improve the manuscript.

Reviewer #2:

The paper is about characterization of ashes of incinerated meat and bone meal (MBM) and poultry litter, as well as phosphorus leaching from the ashes using sulfuric acid or nitric acid. I believe that the information can be of interest for the readers and should be published.

Response: We appreciate the reviewer's positive comments.

My comments are as follows:

Page 3, line 37: "Thermal or biological processing disposes of biomass" - consider another formulation of the text

Response: We have revised the text to make the description clearer. See Page 3, line 37 in the revised manuscript.

Page 4, line 73: the forecast for phosphorus reserves lifetime of 50-100 year is not updated. After upgrading the reserves of Morocco and West Sahara in 2010, the estimated static life time has expanded to around 350 years, ignoring any increase in phosphorus demand. See for example: IFDC (2010). World Phosphate Rock Reserves and Resources. International Fertilizer Development Centre. Technical Bulletin T-75. Please incorporate this information into the paper.

Response: We have updated the forecast for phosphorus reserves lifetime according to the information provided by the reviewer. See Page 4, Lines 72-74 in the revised manuscript.

Page 4, line 75: "around 90%" is not correct. 71% of the reported global reserves are under the control of Morocco and West Sahara according to USA Geological Survey 2019.

Response: We have updated the data and description according to the information provided by the reviewer. See Page 4, Lines 75-76 in the revised manuscript.

Page 9, line 193: the text refers to table S1. I don't find the table in the paper

Page 17, line 400: the text refers to Fig S2(a). I don't find the figure in the paper

Page 17, line 401: the text refers to Fig S2(b). I don't find the figure in the paper

Page 17, line 405: the text refers to Fig S3(a). I don't find the figure in the paper

Page 17, line 410: the text refers to Fig S4. I don't find the figure in the paper

Response: This table and these figures are part of the supplementary information (SI) file.

It is not clear if the experiments were performed in replications.

Response: We have indicated the replication of experiments in figure captions where applicable and in Page 9, line 200, and Page 10, Line 216 in the revised manuscript.

Characterisation of ashes from waste biomass power plants and phosphorus recovery

Lijian Leng [a], Anna A. Bogush [b], Amitava Roy [c], Julia A. Stegemann [b *]

[a] *School of Resources, Environmental & Chemical Engineering and Key Laboratory of Poyang Lake Environment and Resource Utilization, Ministry of Education, Nanchang University, Nanchang, 330031, China*

[b] *Centre for Resource Efficiency & the Environment, Department of Civil, Environmental & Geomatic Engineering, University College London, Chadwick Building, Gower Street, London WC1E 6BT, UK*

[c] *J. Bennett Johnston, Sr., Center for Advanced Microstructures & Devices, Louisiana State University, 6980 Jefferson Hwy, Baton Rouge, LA 70806, USA*

[*] *Corresponding author. Tel.: +44 (0)2076797370*

E-mail address: j.stegemann@ucl.ac.uk (J.A. Stegemann)

Abstract: Biowastes, such as meat and bone meal (MBM), and poultry litter (PL), are used as energy sources for industrial combustion in the UK. However, the biomass ashes remaining after combustion, which contain nutrients such as phosphorus, are landfilled rather than utilised. To promote their utilisation, biomass ashes from industries were characterised in terms of their elemental and mineral compositions, phosphorus extractability, and pH-dependent leachability. These ashes were highly alkaline (pH as high as 13), and rich in calcium and phosphorus. The P bio-availabilities in the ash evaluated by Olsen's extraction were low. Hydroxyapatite and potassium sodium calcium phosphate were identified by X-ray powder diffraction (XRD) as the major phases in the MBM and PL ashes, respectively. The leaching of P, Ca, and many other elements was pH dependent, with considerable increase in leaching below about pH 6. P recovery by acid dissolution (e.g., with H_2SO_4) seems feasible and promising; the optimized acid consumption for ~90% P recovery could be as low as 3.2-5.3 mol H^+/mol P.

Keywords: incineration; fertiliser; phosphorus recovery; acid neutralisation capacity; animal manure

1. Introduction

Thermal or biological processing of biomass produces heat, electricity, or liquid/gas/solid bioenergy with low net greenhouse gas emissions (Ragauskas, 2006). Wood and wood wastes, agricultural crops and their waste byproducts, animal wastes, wastes from food processing, aquatic plants, and algae are the most widely used biomass energy resources (Bogush et al., 2018; Demirbas, 2004; Huang and Yuan, 2015; Leng et al., 2018a, 2018b, 2016; Saidur et al., 2011). These biomass resources, which are currently often treated as organic wastes, can contribute significantly to the generation of renewable energy and reduction of greenhouse gas (GHG) emissions, reducing the dependency on fossil fuels (Ragauskas, 2006). The UK, for example, sets a target of 80% GHG emissions reduction over 1990 levels by 2050; the bioenergy industry contributes significantly to the achievement of these goals (Adams et al., 2011).

Consequently, recovery of energy from biomass by combustion or production of fuel, e.g., from straw, meat and bone meal, poultry litter, wood shavings, and horse bedding, is increasing in the UK, due to the mounting production of these wastes, their energy contents, and the environmental benefits of their utilisation (Oshita et al., 2016; Williams et al., 2016). However, management of ash has emerged to be one of the problems impeding the development of biomass combustion for energy (Niu et al., 2016). Since biomass ashes are rich in the nutrients phosphorus and potassium, they have been considered for use as a soil amendment on agricultural land. However, the low P availability, high alkalinity (e.g., pH 13 or higher), and heavy metal contents in these ashes may restrict their direct application (Niu et al., 2016; Vassilev et al., 2013a; Bogush et al., 2018). Environmental pollution from nutrient and contaminant leaching can occur, and result in negative effects on crops, soils and water, when

ashes are applied under soil and climatic conditions that increase environmental mobility of contaminants (Pettersson et al., 2008a; 2008b), or mobilise nutrients but do not favour their agronomic utilization, e.g., due to excessive application or an imbalance in the nutrient proportions (Bolan et al., 2010; Codling et al., 2002; Szögi et al., 2015; Williams et al., 2016). However, it is worth mentioning that environmental pollution by nutrients and contaminants has also been observed for soil fertilized with animal residues (e.g., pig slurry) directly (Cela et al., 2010; Gunkel-Grillon et al., 2015; Olson et al., 2010).

Meanwhile, the widespread global use of P fertiliser over the past century and increasing demand for P by agriculture threatens to deplete sources of P-bearing rock within the next century (Cordell et al., 2009; 2010; Mayer et al., 2016; Sattari et al., 2012; Tilman et al., 2001; Tilman and Lehman, 1987). Even ignoring rapidly increasing P demand, the estimated static lifetime of phosphorus reserves is only around 350 years (IFDC, 2010). Furthermore, the remaining reserves are highly geographically concentrated (Elser and Bennett, 2011), with around 71% located in Morocco and Western Sahara (USGS, 2019). Therefore, sourcing P from the P consumption lifecycle and developing appropriate P recovery technology, especially in places with a scarcity of natural P-bearing rock such as the UK, is important to meet the increasing demand for this element (Cooper, 2014; Cordell et al., 2011; Mayer et al., 2016; Rittmann et al., 2011). Phosphorus recovery from animal residues (e.g., poultry litter, meat and bone meal) and sewage sludge, and their incineration ashes, is one of the most promising ways to increase the P resource security and secure future food production (Akinola, 2013; Bogush et al., 2018; Havukainen et al., 2016; Kleemann et al., 2015; Mayer et al., 2016; Tan and Lagerkvist, 2011). Cooper and Carliell-Marquet (2013) estimated that the P recovery potential from animal

manure produced in the UK could be higher than national net total P imports; in general, the P value of meat and bone meal/animal bone alone is likely of a similar order of magnitude to that of a country's phosphate fertiliser imports (Cooper and Carliell-Marquet, 2013; Simons et al., 2014).

Hence, recovery of P from biomass ashes to produce more effective and environmentally benign P fertilizer is of increasing interest for both research and practice. Animal manures and manure derivatives such as ash and char have been widely explored for P recovery, with measurement of varied recovery rates and acid demands because of differences between the sources (e.g., P concentration 4.0-139 g kg^{-1}) and process conditions (e.g., different acid types and loads, and solid/liquid ratios) (Table 1). For example, P recovery rates around 90% were obtained for animal manure char, but at acid loads in the region of 100 mol H^+/mol P recovered (Azuara et al., 2013; Heilmann et al., 2014). Lower acid loads (3-10 mol H^+/mol P recovered) were found effective for P recovery from manures and their ashes (Cohen, 2009; Kaikake et al., 2009; Kuligowski and Poulsen, 2010), which is similar to the recovery rates and acid loads for P recovery from sewage sludge ash (Petzet et al., 2012). In addition to P content and recovery conditions, P speciation in the different P-containing resources (wastes) also influences P recovery performance. Elemental, mineral and chemical compositions have been used to describe P speciation in these materials (Bogush et al., 2018; Vassilev et al., 2013a, 2013b, 2013c), but few studies have related these results to P recovery performance. Furthermore, little has been reported regarding meat and bone meal (MBM) and its derivatives (e.g., ash), despite the high P recovery potential from these materials.

The main objectives of this research were thus:

1) to characterise biomass ashes from combustion of MBM or co-combustion of

poultry litter (PL) in UK biomass power plants (https://biofuelwatch.org.uk/wp-content/maps/uk-biomass.html), and

2) to examine the potential and options for P recovery from these biomass ashes.

The bioavailability of P from biomass ashes and potential for its recovery from the biomass ashes depends on P speciation and matrix composition. The biomass ashes were therefore characterised by multiple techniques, including elemental analysis, thermogravimetric analysis (TGA), determination of crystalline phases by X-ray powder diffraction (XRD), characterization of functional groups by Fourier transform infrared spectroscopy (FTIR), and measurement of acid neutralization capacity (ANC) and pH-dependent P leachability, to understand the mechanisms responsible for control of P solubility. P K-edge X-ray absorption near edge spectroscopy (XANES) was used to examine the speciation of P in complex matrices without interference from irrelevant phases and irrespective of crystallinity.

2. Materials and methods

2.1 Materials

Five samples of biomass ash were collected from four different industrial-scale biomass power plants in the UK that use different biomass types as the energy source. The plants use moving grate incinerators with a combustion temperature of 850 ^{o}C, dry discharge of bottom ash, and dry scrubbing of the flue gas. MBM1-BA and MBM2-BA were bottom ashes collected from two different plants that combust MBM; MBM2-APCr was the fly ash from the second plant. PL1-BA and PL2-BA were both bottom ashes from different power plants that co-combust PL. The moisture contents of the biomass ashes were negligible (Bogush et al., 2018). The samples were ground to < 250 µm using a ball mill and then stored in air-tight containers before use.

Reference materials used in the mineralogical investigation included a Ward's

Science Apatite Research Mineral (www.wardsci.com; Catalogue No. 470026-560), a Moroccan apatite (carbonate apatite), and brushite ($CaHPO_4 \cdot 2H_2O$, 99.0%, Sigma-Aldrich).

2.2 Biomass ash elemental composition and bioavailability of P

The biomass ashes were subjected to total digestion using HNO_3: $HClO_4$: H_2O_2 (v, 30%) = 5:5:3, v/v) (Leng et al., 2014) before chemical analysis for the elements of interest (Section 2.7). Separate extracts for P analysis (Section 2.7) were prepared by digestion with potassium persulfate at 150^{o}C for 4.0 h.

Olsen's method has been widely used to evaluate the bioavailability of phosphorus (Olsen et al., 1954). The extraction was conducted in triplicate for all of the biomass samples and residues from leaching at mildly acidic pH (Section 2.5) by mixing 2.5 g ash with 50 mL 0.5 M of sodium bicarbonate (pH 8.5) and shaking for 30 min before separation of the extracts for analysis (Section 2.7).

2.3 Biomass ash mineralogy

The crystalline phases present in the biomass ashes and residues after leaching at mildly acidic pH (Section 2.5) were identified by XRD analysis on an XPERT-PRO diffractometer with an X-ray source of Cu K_α radiation at 40 KV and 30 mA. A scanning speed of 4 s per step and step size of 0.05° (2θ) were used in the scanning range of 5°–70° (2θ). The XRD data were analysed by using Jade software version 6.0 (Materials Data Inc., Livermore, USA).

Fourier transform infrared spectra (FTIR) of the biomass ashes, residues, and reference materials were obtained on a Thermo-Fischer Scientific Nicolet 670 spectrometer in the wavelength range of 400–4000 cm^{-1}.

Thermogravimetric analysis of the biomass ashes, residues, and reference materials was conducted by heating from room temperature to 1000 ^{o}C at a rate of 10 ^{o}C/min

under nitrogen atmosphere.

2.4 Phosphorus speciation

The speciation of P in the biomass ashes and residues after leaching at mild acidic pH (Section 2.5) was assessed by comparing their P K-edge X-ray absorption near edge structure (XANES) spectra with those of the reference materials. P K-edge measurements were made at the Low Energy X-ray Absorption Spectroscopy (Lexas) beamline of Louisiana State University's synchrotron research facility, the J. Bennett Johnston, Sr. Center for Advanced Microstructures and Devices (CAMD), USA. Lexas is a windowless beamline, i.e., with only a 13 µm think Katon™ window separating the ring from the experimental chamber. A University of Bonn-designed Lemonnier type monochromator with InSb 111 crystals was used in measurements. The measurements were made in fluorescence by diluting the sample as necessary with boron nitride to reduce self-absorption (Oxmann, 2014). A Ketek 150 mm^2 silicon drift detector was used for fluorescence measurements. The white line of reagent grade aluminum phosphate was used to calibrate the monochromator at 2152.8 eV. The parameters for the measurements were 2050 eV to 2110 eV with 5 eV steps, 2110 eV to 2142 eV with 0.5 eV steps, 2142 eV to 2160 eV with 0.1 eV steps, from 2160 to 2180 eV with 0.5 eV steps, and 2180 eV to 2250 eV with 1 eV steps. The integration time was from 1 to 5 seconds for adequate counting statistics. The spectra were analyzed with Athena in Demeter (Ravel and Newville, 2005).

2.5 pH-dependent leaching

The acid neutralization capacity (ANC) of the biomass ashes was measured to examine their pH responses to acid addition, and the consequent changes in the solubilities of their components of interest. This test involves adding increasing amounts of nitric acid to a series of 10 or more subsamples of the material under

investigation (Stegemann and Côté, 1991). A single series of 5.0 g subsamples was weighed out for each of the biomass ashes and mixed with 30 mL of nitric acid diluted with deionized water to a concentration from 0 to 3 N (up to 18 meq/g of biomass ash) HNO_3. After 48h of end-over-end mixing at 30 rpm, the samples were centrifuged, and the pH values and conductivities of all the supernatants were measured before separation of the leachates for analysis. The solid residues corresponding to leachates with mild acidic pH (6.2, 5.1, 5.9, 6.5, and 6.8 for MBM1-BA, MBM2-BA, MBM2-APCr, PL1-BA, and PL2-BA, respectively (Table S1) were also analysed by XRD (Section 2.3) FTIR (Section 2.3), XANES (Section 2.4), and Olsen's method (Section 2.2) after drying at 60 ^{o}C.

2.6 Acid extraction for phosphorus recovery

To further assess acid extractability of P from the biomass ashes, the effects of contact time (0-48 h), liquid/solid ratio (4-20 mL/g of ash), acid type (HNO_3 and H_2SO_4), and acid load (6-16 meq H^+/g ash) were investigated with the volume of the extraction liquid fixed at 30 mL. Experiments were conducted in duplicate. P recovery rate was defined as the percentage of P in the leachate as compared with that in the original ash.

2.7 Chemical analysis of extracts and leachates

Liquid samples from digestion, extraction, and wastewater treatment were filtered from the solids through 0.45 µm membrane filters; leachates for metal analysis were acidified to pH 2 before storage.

P in the filtered liquid samples was determined by colorimetry at 880 nm, by reaction with ammonium molybdate using ascorbic acid as the reducing agent (Murphy and Riley, 1962).

Metals, including Al, B, Bi, Ba, Ca, Co, Cr, Cu, Cd, Fe, K, Mg, Li, Mn, Na, Ni, Pb,

Sr, and Zn, and P in the extracts from total digestion of the biomass ashes and the ANC test leachates were determined by Inductively Coupled Plasma Optical Emission Spectroscopy (ICP-OES).

Anions in the ANC leachates, including F^-, Cl^-, Br^-, NO_2^-, NO_3^-, PO_4^{3-} and SO_4^{2-}, were analysed by a Dionex AQUION Ion Chromatography (IC) before acidification of the samples.

All chemical analyses were conducted in triplicate with reporting of mean values.

3. Results and discussion

3.1 Biomass ash elemental composition and bioavailability of P

The elemental compositions of the biomass ashes in Table 2 are typical for ashes from animal residue incineration (Bogush et al., 2018; Oshita et al., 2016; Vassilev et al., 2012; Zhang et al., 2002). Apart from P, the major elements are Al, Fe, K, Mg, Mn, and Na, with Ca as the most abundant element comprising 16-32% of the total ash.

The P concentrations of these ashes range from 8.3-13%, which is comparable to that of some natural phosphorus rocks [e.g., 30–40% P_2O_5; 13–17.5% P (Desmidt et al., 2015; Elouear et al., 2008)]. However, Fig. 2 shows that the contents of bioavailable P in the ashes are less than 800 mg P/kg ash, corresponding to <0.7% of the total P.

The contents of K and, especially, Mg, in the PL ashes are higher than those of the MBM ashes. Some differences between the compositions of ashes from different MBM incineration plants can also be observed, e.g., MBM1-BA has higher contents of Ca and P, and lower contents of K and Na compared to MBM2-BA, showing the effects of variations in the original MBM materials. Minor elements such as B, Zn, Sr, Ba, and Cu are in the range of 100-1100 mg/kg, while trace elements such as Bi, Cd,

Cr, Co, Li, Ni, and Pb are <100 mg/kg.

3.2 Biomass ash mineralogy

Fig. 1(a) shows that the dominant phase identified in the MBM ashes by XRD is hydroxyapatite (HAP), which is consistent with the high contents of Ca and P. Hydroxyapatite, with some carbonation, is the principal mineral in bone (e.g., Elliott, 2002), and increases in crystallinity with heating. Both β-tricalcium phosphate [β-$Ca_3(PO_4)_2$, β-TCP] and HAP were identified by XRD as the major phases in either dried or calcined bones (Brod et al., 2015; Rajendran et al., 2013). XRD identified potassium sodium calcium phosphate [$KNaCa_2(PO_4)_2$] as the main phase in the PL ashes. This phase is also identified as the major mineral phase after combustion of P and Ca-bearing biomass at a temperature of 815 ^oC (Kongsomart et al., 2016). The solubility of apatite varies significantly depending on its content of other anions (e.g., CO_3^{2-}, Cl^- or F^-) (Magalhães and Williams, 2007), but $Ca_5(PO_4)_3(OH)$, which has K_{sp} = 3.98×10^{-59} (Chow, 2001; Delvasto et al., 2006) might be expected to have low bioavailability, as was observed for the biomass ashes (Section 3.1). No data about bioavailability was found for $KNaCa_2(PO_4)_2$.

A comparison of the Moroccan apatite FTIR spectrum with those of the ashes [Fig. 1(b)] shows that all are dominated by the ca. 1030 cm^{-1} (anti-symmetric stretch Υ_3) band, with the Υ_1 (ca. 960 cm^{-1}) and symmetric stretch Υ_4 bands (F_2 bend 650-525 cm^{-1}) also being conspicuous; the resemblance to the reference material is most obvious for MBM1-BA and MBM2-APCr. However, all phosphate bands show some shift, indicating variations in composition, e.g., substitution of CO_3^{2-} in the crystal structure. The CO_3^{2-} ion can be found in the channels (A type) of the hexagonal crystal structure of apatite, or substitutes for the phosphate ion (B type). With B type carbonate apatite, there is a doublet around 1430 cm^{-1} (Fleet, 2009), as seen in the

Moroccan apatite. PL1-BA thus seems to contain carbonate apatite whereas the other ashes showed only hydroxyapatite. The OH^- peak at 3420 cm^{-1} in all FTIR spectra is quite weak, but the derivative thermogravimetric (DTG) curves [Fig. 1(c)] show that all ashes have mass loss peaks in the region 200 °C to 400 °C. A comparison with apatite standards used in this study (not shown) and data from the literature suggests this peak is from the OH in the apatite in the ashes. The DTG curves also have doublets, which vary in strength depending on the biomass ash, in the region 600°C to 800°C, one of which is likely from the carbonate in the apatite structure, whereas the other one is calcium carbonate (Peters et al., 2000).

Previous studies have also found hydroxyapatite and $KNaCa_2(PO_4)_2$ (Bogush et al., 2018; Coutand et al., 2008; Komiyama et al., 2013; Oshita et al., 2016; Sugiyama et al., 2016), but also other minerals, e.g., $Ca_3(PO_4)_2$ in ashes from MBM or animal manure combustion (Coutand et al., 2008; Sugiyama et al., 2016) and $Ca_9MgK(PO_4)_7$ in manure ashes (Komiyama et al., 2013; Oshita et al., 2016).

XRD also showed portlandite [$Ca(OH)_2$] in the MBM ashes, which is corroborated by the 3643 cm^{-1} FTIR band, suggestive of OH^- in $Ca(OH)_2$ for all ashes but PL1-BA. The single similar carbonate band around 1430 cm^{-1} (Υ_3) in the FTIR spectra of all ashes except PL1-BA is typical of calcite, corresponding to calcite ($CaCO_3$) peaks in the XRD patterns except PL ashes.

XRD indicates sulphate to be present as calcium sulphate ($CaSO_4$) in all MBM ashes (Table 3), and arcanite (K_2SO_4) in the MBM2 and PL ashes. The FTIR spectra of MBM2-BA and PL2-BA are unlike those of the other ashes due to higher amounts of arcanite, which presents as peaks at 618 cm^{-1}, 1100 cm^{-1} and 1197 cm^{-1}. Sulfate breakdown may be responsible for the peak observed in the DTG at 931°C (MBM2-APCr).

XRD also shows quartz (SiO_2) in the PL ashes and MBM1-BA, and abundant halite (NaCl) in MBM2-APCr and MBM2-BA.

3.3 Phosphorus speciation

Fig. 1(d) shows the phosphorus K-edge XANES spectra of the samples along with that of the Ward's Science apatite. The white line position (A) of the latter is 2151.84 eV, while that of the ash samples ranges from 2151.67 eV to 2151.85 eV. The phosphate white line is from resonance between 1s and higher energy t_2* orbitals, while the peak around 2168 eV is from the P-O bond. The location and intensity of the C and D maxima depend on the composition and crystallinity of the phosphate phases (Ingall et al., 2011). These ashes thus have different phosphate compositions. Linear combination fitting of the spectrum of the MBM1-BA ash shows it to be principally composed of apatite, but the fit of apatite was not as good for the other ashes. The inflection of the shoulder at ~2155 eV correlates with the Ca/P ratio of the structure (Franke and Hormes, 1995); consequently, the PL ashes, which are indicated by XRD to contain $KNaCa_2(PO_4)_2$, appear to have a lower Ca/P ratio than the MBM ashes, in which $Ca_5(PO_4)_3(OH)$ was identified as the main P-bearing mineral.

There are some contradictions when comparing mineralogy results obtained from different analytical techniques. The variance between mineralogical analyses can be expected when applying different techniques to very small samples, particularly for complex materials such as these. Mineral phases identified by XRD were used in the following discussions unless specified otherwise.

3.4 pH dependent leaching and characterisation of the leached residues

The leachate pH values resulting from the discrete acid loading (on the secondary ordinate in Figs. 3 and 4) suggest a small, near vertical, plateau corresponding to neutralisation of the abundant $Ca(OH)_2$ in the MBM ash at pH ~12; this plateau is

311 absent for the PL ashes, which contain little $Ca(OH)_2$ (section 3.2).

312 A second pH plateau at ~7 may be attributable to several different phenomena.
313 Dissolution of the small component of calcite in the ashes, which will yield a pH
314 lower than that of 8.3 expected in equilibrium with the atmosphere since the leaching
315 tubes are sealed, likely contributes to this plateau. For the MBM ashes, the plateau
316 also reflects dissolution of $Ca_5(PO_4)_3(OH)$, which has an equilibrium pH of ~7.5
317 (based on the K_{sp} noted above). Perhaps most importantly, a phosphate buffer system
318 will result from dissolution of the apatite, and, especially, $KNaCa_2(PO_4)_2$. The second
319 plateau is more apparent for the PL ashes, which had an acid neutralization capacity
320 of 9-10 meq H^+/g to pH 4, whereas it was only 5-6 H^+ meq/g for the MBM ashes.
321 There is a third pH plateau, below pH 4.

322 Fig. 3 shows that sulfate, released at high pH by dissolution of K_2SO_4, drops in
323 concentration below pH 8, likely due to precipitation of gypsum ($CaSO_4 \cdot 2H_2O$; K_{sp} =
324 2.62×10^{-5}; Harouaka et al., 2014), as Ca enters solution from calcite and the
325 phosphate minerals (Fig. 4). Since there is little K_2SO_4 to dissolve from MBM1-BA,
326 Ca is not precipitated and its leached concentration is therefore higher than for the
327 other ashes.

328 Fig. 3 shows constant concentrations of chloride regardless of pH for each
329 biomass ash, consistent with the presence of NaCl identified by XRD. Na and K are
330 also initially released from NaCl and K_2SO_4, but their concentrations rise slightly as
331 the pH falls in the MBM ash leachates, and increase dramatically below pH 8 in the
332 PL ash leachates. P (Fig. 4, and phosphate, Fig. 3) concentrations are seen to be low
333 above pH ~4, and then increase as the phosphate minerals dissolve with further acid
334 addition. Release of Na and K with P from dissolution of the $KNaCa_2(PO_4)_2$ in the PL
335 ashes would be expected, but the increases in their concentrations before the

concentration of P starts to rise suggest that the dissolution of $KNaCa_2(PO_4)_2$ is incongruent, with selective loss of K and Na, or that this mineral dissolves and reprecipitates, e.g., as brushite ($CaHPO_4 \cdot 2H_2O$) (Johnsson and Nancollas, 1992).

Mg, Ba and Sr (Fig. S1) seem to be mainly released in association with the pH~7 plateau. They may substitute for Ca in calcite or phosphate minerals and are released when those dissolve. Cu and Zn form phosphates of low solubility and are mainly released below pH 4; the leaching rates of these elements were undetectable or at very low level at pH 8-12 from MBM1-BA (Fig. S1), because of the relatively low total contents of minor elements in this ash (Table 2). The concentrations of Fe were almost undetectable, and those of Al were negligible, in the leachates from the MBM ashes and PL2-BA. Iron oxides have low solubility, and it is possible that $Fe_3(PO_4)_2 \cdot 8H_2O/FePO_4$, $AlPO_4$, $Pb_5(PO_4)_3(OH)/Pb_3(PO_4)_2$, and $Zn_3(PO_4)_2$, which have low solubility, may exist in the original ashes or were formed as secondary precipitates during the test (Deydier et al., 2003; Parhi et al., 2006; Wilfert et al., 2015).

XRD of the residues in Fig. 1(a) from leaching at mildly acidic pH (5.1-6.8; Section 2.5) shows precipitation of $CaHPO_4 \cdot 2H_2O$ [$K_{sp} = 2.57 \times 10^{-7}$; (Chow, 2001)], which forms under acidic conditions (Johnsson and Nancollas, 1992). Dorozhkin's dissolution mechanism for hydroxyapatite (Eqs. 1–3) demonstrates that $Ca_5(PO_4)_3(OH)$ would produce $Ca_3(PO_4)_2$ ($K_{sp} = 3.16 \times 10^{-26}$ for α-$Ca_3(PO_4)_2$ and $K_{sp} = 1.26 \times 10^{-29}$ for β-$Ca_3(PO_4)_2$ (Chow, 2001)) at the first stage and then addition of additional acid would yield metastable $CaHPO_4$, and finally the dissolution of $CaHPO_4$ (Dorozhkin, 2012; 1997). Brushite solubility can markedly rise with a decrease in pH from 6 to 3 (Kuz'mina et al., 2013) and at lower pH it dissolves linearly (Figs. 3 and 4).

$$2Ca_5(PO_4)_3(OH) + 2H^+ \rightarrow 3Ca_3(PO_4)_2 + Ca^{2+} + 2H_2O \quad (1)$$

$$Ca_3(PO_4)_2 + 2H^+ \rightarrow 2CaHPO_4 + Ca^{2+} \quad (2)$$

$$CaHPO_4 + H^+ \rightarrow H_2PO_4^- + Ca^{2+} \quad (3)$$

The presence of $CaHPO_4 \cdot 2H_2O$ in the residues after leaching at mildly acidic pH (pH 5.1-6.8) was verified by multiple techniques. Fig. 1(a) shows that it dominates the XRD patterns of the leached residues, while the peak intensities for $Ca_5(PO_4)_3(OH)$ in MBM ashes are reduced and $KNaCa_2(PO_4)_2$ in PL ashes have almost disappeared. The prominent peak around 1650 cm^{-1} found in the FTIR spectra of all the leached residues as seen in [Fig. 1 (b)] corresponds to the molecular H_2O peak from $CaHPO_4 \cdot 2H_2O$ at 1645.48 cm^{-1}. The precipitation of $CaHPO_4 \cdot 2H_2O$ is also evident in the DTG traces for the leached residues of all the ashes as a peak at ~183°C [Fig. 1 (c)], with the amount ranging from 21.6-24.2%. Finally, the P K-edge XANES spectra [Fig. 1(d)] confirm that different phosphate phases are present in the leached residues than the original ashes, although fitting to estimate the exact P composition is difficult as several phosphate phases are present. Although $CaHPO_4 \cdot 2H_2O$ ($K_{sp} = 2.57 \times 10^{-7}$) in the residues is more soluble than $Ca_5(PO_4)_3(OH)$ ($K_{sp} = 3.98 \times 10^{-59}$), the bioavailable P in the solid residues separated from the mildly acidic leachates remained low at <1400 mg P/kg ash (Fig. 2). It is noteworthy that $CaHPO_4 \cdot 2H_2O$ can transform back to $Ca_5(PO_4)_3(OH)$ or $Ca_3(PO_4)_2$ in an alkaline and calcium-rich environment (Štulajterová and Medvecký, 2008).

During leaching, the water-soluble NaCl, K_2SO_4, and acid-soluble calcite and $Ca(OH)_2$ were not found in the leached residues, as shown in Fig. 1(a), but gypsum ($CaSO_4 \cdot 2H_2O$) and SiO_2 remained, as they are acid-insensitive over the pH range studied. The absence of the 618 cm^{-1} and 1195 cm^{-1} bands in the FTIR spectra of the leached residues [Fig. 1(b)] indicate the dissolution of the sulfate phases. The 713 cm^{-}

[1] carbonate band from calcite is very weak to non-existent in the residues [Fig. 1(b)]. In the thermogravimetric analysis of the leached residues, all the mass loss occurred by 600°C, and the absence of a calcite peak [Fig. 1(c)] reflect complete dissolution of calcite at the lower pH.

To summarize, NaCl and K_2SO_4 present in ashes dissolved readily with water leaching. Other chemical components dissolved with decreasing pH or increasing acid addition. Alkaline $CaCO_3$ and $Ca(OH)_2$ were neutralized at the first plateau and followed by the dissolution of $Ca_5(PO_4)_3(OH)$ and $KNaCa_2(PO_4)_2$ to produce $CaHPO_4 \cdot 2H_2O$ at pH~7, which continued to dissolve with releasing of P to the leachate from pH ~4. Mg, Ba and Sr mainly released in association with the pH~7 plateau while the release of Fe, Al, Zn, and Cu became evident at pH~4.

3.5 Phosphorus recovery from biomass ash

P release in the ANC test can be used to estimate the P recovery potential from the biomass ashes studied. Phosphorus recovery was found to be linearly dependent on the leachate pH below pH~4, attaining 40-50% at pH~3, and ~100% P recovery at pH~1 [Fig. S2(a)]. Determination of the acid consumption per unit of P recovered [Fig. S2(b)] is essential to assess the economic feasibility of the recovery process, and ranged from 9-14 meq H^+/g ash, assuming that the other ashes follow the trend established to 100% recovery for PL1-BA.

Investigation of the contact time showed that P recovery reached 75-95% of its highest value within several minutes [Fig. S3(a)], but the pH needed several hours to reach steady state [Fig. S3(b)]. This implies that P could be recovered promptly before surplus acid is consumed by the solid ash residue.

Solid/liquid (S/L) ratio also plays a significant role in P recovery; less acid was consumed per unit of P recovered at lower S/L ratios because of more efficient mixing

411 (Fig. S4). For example, results show that 10-20% less acid will be needed at S/L ratio
412 of 0.05, than at a S/L of 0.1, which is the ratio that has been widely used for P
413 dissolution from biomass ashes (Oshita et al., 2016; Sugiyama et al., 2016).
414 Unfortunately, a lower S/L ratio also produces a larger amount of leachate with a
415 lower P concentration, which could make the recycling of P and the subsequent
416 wastewater treatment much more difficult.

417 HNO_3 and H_2SO_4 were therefore applied at S/L 0.1, with a contact time of 2h, to
418 assess the influence of the acid type on P recovery and acid consumption. H_2SO_4
419 seems to be more efficient for P leaching from these biomass ashes compared with
420 HNO_3 particularly at lower acid load (Fig. 5). During the H_2SO_4 process, the
421 precipitation of gypsum promotes the dissolution of apatite, and facilitates the
422 separation of the product. By comparison, separation of dissolved $Ca(NO_3)_2$ formed
423 during HNO_3 leaching is difficult. At H_2SO_4 load of 14 meq H^+/g ash, the acid
424 consumption is in the range of 3.2-5.3 mol H^+/mol P (Fig. 5), which is comparable
425 with those reported in previous studies when animal manures or their derivatives (e.g.,
426 ashes) (Table 1) or sewage sludge ashes (Petzet et al., 2012) were used for P recovery.
427 Meanwhile, P recovery of ~90% or higher was achieved at this acid load.

428 *3.6 Economic considerations*

429 In the phosphorus industry, phosphoric acid is the basic starting raw material for
430 production, which is normally produced from phosphate rock. The wet process is the
431 most commonly used phosphoric acid production process, in which H_2SO_4 dissolves
432 $Ca_5(PO_4)_3(F, Cl, OH)$, followed with purification and condensation to produce
433 phosphoric acid (H_3PO_4) and byproduct phosphogypsum (Tayibi et al., 2009).
434 $Ca_5(PO_4)_3F$ is the dominant component of natural phosphate rock and its dissolution
435 mechanisms during wet-process phosphoric acid production can be described by Eqs.

436 4-7 (Dorozhkin, 1996), which are similar to those for $Ca_5(PO_4)_3(OH)$ (Eqs. 1-3). The
437 overall reaction can be described by Eq. 8 (Wu et al., 2018).

438 $2Ca_5(PO_4)_3(F, OH) + 2H^+ \rightarrow 3Ca_3(PO_4)_2 + Ca^{2+} + 2HF, H_2O$ (4)

439 $Ca_3(PO_4)_2 + 2H^+ \rightarrow 2CaHPO_4 + Ca^{2+}$ (5)

440 $CaHPO_4 + H^+ \rightarrow H_2PO_4^- + Ca^{2+}$ (6)

441 $H_2PO_4^- + H^+ \rightarrow H_3PO_4$ (7)

442 $Ca_{10}(PO_4)_6(F, OH)_2 + 10H_2SO_4 + nH_2O \rightarrow 10CaSO_4 \cdot nH_2O + 6H_3PO_4 + 2HF, H_2O$ (8)

443 The theoretical acid consumption for the wet-process phosphoric acid production
444 is 3.3 mol H^+/mol P or 1.67 mol H_2SO_4/mol H_3PO_4. If the final product is $H_2PO_4^-$, the
445 consumption drops to 2.3 mol H^+/mol P, which is the lowest acid addition needed to
446 dissolve all P into the aqueous phase. However, the processes described by Eqs. 6 and
447 7 proceed at the same time; thus, the lowest theoretical acid consumption for P
448 dissolution from $Ca_5(PO_4)_3(F, OH)$ would be 2.3-3.3 mol H^+/mol P. Considering the
449 presence of minerals such as $CaCO_3$, $MgCO_3$, CaO, and MgO in natural phosphate
450 rock, the consumption would be >2.3-3.3 mol H^+/mol P depending on the content of
451 acid-consuming components, which is comparable to that of dissolution of MBM
452 ashes (3.2-4.2 mol H^+/mol P). Furthermore, the dissolution of MBM ashes (composed
453 of $Ca_5(PO_4)_3(OH)$) would not be complicated by the presence of fluorine, which is
454 abundant in phosphate rock. Therefore, P recovery from MBM ashes by direct acid
455 dissolution seems very promising and worth further investigation.

456

457 **4. Conclusions**

458 Hydroxyapatite [$Ca_5(PO_4)_3(OH)$] and potassium sodium calcium phosphate
459 [$KNaCa_2(PO_4)_2$] seem to be the main mineral phases in the MBM and PL ashes,
460 respectively, with low bioavailability of P. Phosphate leaching is pH dependent and

significant recovery was experienced at pH <4. Major heavy metals such as Cu and Zn demonstrated similar leaching behavior as P. A substantial proportion of the P remaining in the solid residues after acid leaching was transformed to brushite, but its bioavailability increased only slightly.

It appears that secondary P, for industrial production of fertilizer or other chemicals, could be recovered from MBM and PL ashes by acid dissolution (particularly by H_2SO_4), with acid consumption as low as 3.2-5.3 mol H^+/mol P and up to 90% P recovery. Particularly, the consumption when recovering P from MBM (3.2-4.2 mol H^+/mol P) is close to that required for P recovery from natural phosphate rock.

Acknowledgment

The research was financially supported by the British Council (Newton Fund) and the China Scholarship Council [File No. 201503780024]. The authors wish to thank Dr. Judith Zhou for helping with the IC analysis, Catherine Unsworth for running the ICP-OES analysis, and Dr. Shi Shi for carrying out the XRD analysis. We also gratefully acknowledge the biomass fuel plants, who chose to be anonymous, for providing the ash samples.

References

Adams, P.W., Hammond, G.P., McManus, M.C., Mezzullo, W.G., 2011. Barriers to and drivers for UK bioenergy development. Renew. Sustain. Energy Rev. 15, 1217–1227. doi:10.1016/j.rser.2010.09.039

Akinola, O., 2013. Overview of Phosphorus Recovery and Recycling From Selected Waste Streams - Protecting Phosphorus as a Resource. Imperial College London.

Azuara, M., Kersten, S.R.A., Kootstra, A.M.J., 2013. Recycling phosphorus by fast pyrolysis of pig manure: Concentration and extraction of phosphorus combined with formation of value-added pyrolysis products. Biomass Bioenerg. 49, 171–180. doi:10.1016/j.biombioe.2012.12.010

Bogush, A.A., Stegemann, J.A., Williams, R., Wood, I.G., 2018. Element speciation in UK biomass power plant residues based on composition, mineralogy, microstructure and leaching. Fuel 211, 712–725. doi:10.1016/j.fuel.2017.09.103

Bolan, N.S., Szogi, A.A., Chuasavathi, T., Seshadri, B., Rothrock, M.J., Panneerselvam, P., 2010. Uses and management of poultry litter. Worlds. Poult. Sci. J. 66, 673–698. doi:10.1017/S0043933910000656

Brod, E., Øgaard, A.F., Hansen, E., Wragg, D., Haraldsen, T.K., Krogstad, T., 2015. Waste products as alternative phosphorus fertilisers part I: inorganic P species affect fertilisation effects depending on soil pH. Nutr. Cycl. Agroecosystems 103, 167–185. doi:10.1007/s10705-015-9734-1

Cela, S., Berenguer, P., Santiveri, F., Lloveras, J., 2010. Potential phosphorus, potassium, and magnesium surpluses in an irrigated maize monoculture fertilized with Pig slurry. Agron. J. 102, 96–102. doi:10.2134/agronj2009.0139

Chow, L.C., 2001. Solubility of Calcium Phosphates. Octacalcium Phosphate l, 94–111. doi:10.1159/000061650

Cohen, Y., 2009. Phosphorus dissolution from ash of incinerated sewage sludge and animal carcasses using sulphuric acid. Environ. Technol. 30, 1215–1226. doi:10.1080/09593330903213879

Cooper, J., 2014. Managing phosphorus in the UK water industry to increase national resource security. The University of Birmingham.

Cooper, J., Carliell-Marquet, C., 2013. A substance flow analysis of phosphorus in the UK food production and consumption system. Resour. Conserv. Recycl. 74, 82–100. doi:10.1016/j.resconrec.2013.03.001

Cordell, D., 2010. The story of phosphorus: Sustainability implications of global phosphorus scarcity for food security. Linköping University.

Cordell, D., Drangert, J.O., White, S., 2009. The story of phosphorus: Global food security and food for thought. Glob. Environ. Chang. doi:10.1016/j.gloenvcha.2008.10.009

Cordell, D., Rosemarin, A., Schroder, J.J., Smit, A.L., 2011. Towards global phosphorus security: A systems framework for phosphorus recovery and reuse options. Chemosphere 84, 747–758. doi:10.1016/j.chemosphere.2011.02.032

Coutand, M., Cyr, M., Deydier, E., Guilet, R., Clastres, P., 2008. Characteristics of industrial and laboratory meat and bone meal ashes and their potential applications. J. Hazard. Mater. 150, 522–532. doi:10.1016/j.jhazmat.2007.04.133

Delvasto, P., Valverde, A., Ballester, A., Igual, J.M., Munoz, J.A., Gonzalez, F., Blazquez, M.L., Garcıa, C., 2006. Characterization of brushite as a re-crystallization product formed during bacterial solubilization of hydroxyapatite in batch cultures. Soil Biol. Biochem. 38, 2645–2654. doi:10.1016/j.soilbio.2006.03.020

Demirbas, A., 2004. Combustion characteristics of different biomass fuels. Prog. Energy Combust. Sci. 30, 219–230. doi:10.1016/j.pecs.2003.10.004

Desmidt, E., Ghyselbrecht, K., Zhang, Y., Pinoy, L., Van der Bruggen, B., Verstraete, W., Rabaey, K., Meesschaert, B., 2015. Global Phosphorus Scarcity and Full-Scale P-Recovery Techniques: A Review. Crit. Rev. Environ. Sci. Technol. 45, 336–384. doi:10.1080/10643389.2013.866531

Deydier, E., Guilet, R., Sharrock, P., 2003. Beneficial use of meat and bone meal combustion residue: “An efficient low cost material to remove lead from aqueous effluent.” J. Hazard. Mater. 101, 55–64. doi:10.1016/S0304-3894(03)00137-7

Dorozhkin, S. V, 2012. Dissolution mechanism of calcium apatites in acids: A review of literature. World J. Methodol. 2, 1–17. doi:10.5662/wjm.v2.i1.1

Dorozhkin, S. V, 1997. Surface Reactions of Apatite Dissolution. J. Colloid Interface Sci. 191, 489–497. doi:10.1006/jcis.1997.4942

Dorozhkin, S. V, 1996. Fundamentals of the Wet-Process Phosphoric Acid Production . 1 . Kinetics and Mechanism of the Phosphate Rock Dissolution. Ind. Eng. Chem. Res. 35, 4328–4335. doi:10.1021/ie960092u

Ekpo, U., Ross, A.B., Camargo-Valero, M.A., Fletcher, L.A., 2016. Influence of pH on hydrothermal treatment of swine manure: Impact on extraction of nitrogen and phosphorus in process water. Bioresour. Technol. 214, 637–644.

Elouear, Z., Bouzid, J., Boujelben, N., Feki, M., Jamoussi, F., Montiel, A., 2008. Heavy metal removal from aqueous solutions by activated phosphate rock. J. Hazard. Mater. 156, 412–420. doi:10.1016/j.jhazmat.2007.12.036

Elser, J., Bennett, E., 2011. A broken biogeochemical cycle. Nature 478, 29–31. doi:10.1038/478029a

Elliott, J. C., 2002. Calcium Phosphate Biominerals. Rev. Mineral. Geochem. 48(1): 427-453.

Fleet, M. E., 2009. Infrared spectra of carbonate apatites: ν2-Region bands. Biomaterials 30(8): 1473-1481.

Franke, R., Hormes, J., 1995. The P K-near edge absorption spectra of phosphates. Phys. B Phys. Condens. Matter 216, 85–95. doi:10.1016/0921-4526(95)00446-7

Grzmil, B., Wronkowski, J., 2006. Removal of phosphates and fluorides from industrial wastewater. Desalination 189, 261–268. doi:10.1016/j.desal.2005.07.008

Gunkel-Grillon, P., Roth, E., Laporte-Magoni, C., Le Mestre, M., 2015. Effects of long term raw pig slurry inputs on nutrient and metal contamination of tropical volcanogenic soils, Uvéa Island (South Pacific). Sci. Total Environ. 533, 339–46. doi:10.1016/j.scitotenv.2015.06.110

Harouaka, K., Eisenhauer, A., Fantle, M.S., 2014. Experimental investigation of Ca isotopic fractionation during abiotic gypsum precipitation. Geochim. Cosmochim. Acta 129, 157–176. doi:10.1016/j.gca.2013.12.004

Havukainen, J., Nguyen, M.T., Hermann, L., Horttanainen, M., Mikkilä, M., Deviatkin, I., Linnanen, L., 2016. Potential of phosphorus recovery from sewage sludge and manure ash by thermochemical treatment. Waste Manag. 49, 221–229. doi:10.1016/j.wasman.2016.01.020

He, Z., Pagliari, P.H., Waldrip, H.M., 2016. Applied and Environmental Chemistry of Animal Manure: A Review. Pedosphere 26, 779–816. doi:10.1016/S1002-0160(15)60087-X

Heilmann, S.M., Molde, J.S., Timler, J.G., Wood, B.M., Mikula, A.L., Vozhdayev, G. V, Colosky, E.C., Spokas, K. a, Valentas, K.J., 2014. Phosphorus Reclamation through Hydrothermal Carbonization of Animal Manures. Environ. Sci. Technol. doi:10.1021/es501872k

Huang, H., Yuan, X., 2015. Recent progress in the direct liquefaction of typical biomass. Prog. Energy Combust. Sci. 49, 59–80. doi:10.1016/j.pecs.2015.01.003

IFDC, 2010. World Phosphate Rock Reserves and Resources. International Fertilizer Development Centre.

Ingall, E. D., Brandes J. A., Diaz J. M., de Jonge M. D., Paterson D., McNulty I., Elliott W.C., Northrup P., 2011. Phosphorus K-edge XANES spectroscopy of mineral standards. J. Synchrotron Radiat 18: 189-197.

Johnsson, M.S.-A., Nancollas, G.H., 1992. The Role of Brushite and Octacalcium Phosphate in Apatite Formation. Crit. Rev. Oral Biol. Med. 3, 61–82. doi:10.1177/10454411920030010601

Kaikake, K., Sekito, T., Dote, Y., 2009. Phosphate recovery from phosphorus-rich solution obtained from chicken manure incineration ash. Waste Manag. 29,

1084–1088. doi:10.1016/j.wasman.2008.09.008
Kleemann, R., Chenoweth, J., Clift, R., Morse, S., Pearce, P., Saroj, D., 2015. Evaluation of local and national effects of recovering phosphorus at wastewater treatment plants: Lessons learned from the UK. Resour. Conserv. Recycl. 105, 347–359. doi:10.1016/j.resconrec.2015.09.007
Komiyama, T., Kobayashi, A., Yahagi, M., 2013. The chemical characteristics of ashes from cattle, swine and poultry manure. J. Mater. Cycles Waste Manag. 15, 106–110. doi:10.1007/s10163-012-0089-2
Kongsomart, B., Kannari, N., Takarada, T., 2016. Catalytic Effects of Biomass-Derived Ash on Loy Yang Brown Coal Gasification. Int. J. Biomass Renewables 5, 12–22.
Kuligowski, K., Poulsen, T.G., 2010. Phosphorus and zinc dissolution from thermally gasified piggery waste ash using sulphuric acid. Bioresour. Technol. 101, 5123–5130. doi:10.1016/j.biortech.2010.01.143
Kuz'mina, M.A., Zhuravlev, S. V., Frank-Kamenetskaya, O. V., 2013. The effect of medium chemistry on the solubility and morphology of brushite crystals. Geol. Ore Depos. 55, 692–697. doi:10.1134/S1075701513080072
Leng, L., Li, J., Wen, Z., Zhou, W., 2018a. Use of microalgae to recycle nutrients in aqueous phase derived from hydrothermal liquefaction process. Bioresour. Technol. 256, 529–542. doi:10.1016/j.biortech.2018.01.121
Leng, L., Li, J., Yuan, X., Li, J., Han, P., Hong, Y., Wei, F., Zhou, W., 2018b. Beneficial synergistic effect on bio-oil production from co-liquefaction of sewage sludge and lignocellulosic biomass. Bioresour. Technol. 251, 49–56. doi:10.1016/j.biortech.2017.12.018
Leng, L., Yuan, X., Huang, H., Jiang, H., Chen, X., Zeng, G., 2014. The migration and transformation behavior of heavy metals during the liquefaction process of sewage sludge. Bioresour. Technol. 167, 144–150. doi:10.1016/j.biortech.2014.05.119
Leng, L., Yuan, X., Shao, J., Huang, H., Wang, H., Li, H., Chen, X., Zeng, G., 2016. Study on demetalization of sewage sludge by sequential extraction before liquefaction for the production of cleaner bio-oil and bio-char. Bioresour. Technol. 200, 320–327. doi:10.1016/j.biortech.2015.10.040
Magalhães, M.C.F., Williams, P.A., 2007. Apatite Group Minerals Solubility and Environmental Remediation, in: Thermodynamics, Solubility and Environmental Issues. pp. 327–340.
Mayer, B.K., Baker, L.A., Boyer, T.H., Drechsel, P., Gifford, M., Hanjra, M.A., Parameswaran, P., Stoltzfus, J., Westerhoff, P., Rittmann, B.E., 2016. Total Value of Phosphorus Recovery. Environ. Sci. Technol. 50, 6606–6620. doi:10.1021/acs.est.6b01239
Murphy, J., Riley, J.P., 1962. A modified single solution method for the determination of phosphate in natural waters. Anal. Chim. Acta 27, 31–36. doi:10.1016/S0003-2670(00)88444-5
Niu, Y., Tan, H., Hui, S., 2016. Ash-related issues during biomass combustion: Alkali-induced slagging, silicate melt-induced slagging (ash fusion), agglomeration, corrosion, ash utilization, and related countermeasures. Prog. Energy Combust. Sci. 52, 1–61. doi:10.1016/j.pecs.2015.09.003
Olsen, S.R., Cole, C. V, Watandbe, F., Dean, L., 1954. Estimation of Available Phosphorus in Soil by Extraction with sodium Bicarbonate. U.S. Dep. Agric. 939.
Olson, B.M., Bremer, E., McKenzie, R.H., Bennett, R., 2010. Phosphorus

accumulation and leaching in two irrigated soils with incremental rates of cattle manure. Can. J. Soil Sci. 90, 355–362. doi:10.4141/CJSS09025
Oshita, K., Sun, X., Kawaguchi, K., Shiota, K., Takaoka, M., Matsukawa, K., Fujiwara, T., 2016. Aqueous leaching of cattle manure incineration ash to produce a phosphate enriched fertilizer. J. Mater. Cycles Waste Manag. 18, 608–617. doi:10.1007/s10163-016-0528-6
Oxmann, J. F., 2014. Technical Note: An X-ray absorption method for the identification of calcium phosphate species using peak-height ratios. Biogeosciences 11(8): 2169-2183.
Parhi, P., Ramanan, A., Ray, A.R., 2006. Hydrothermal Synthesis of nanocrystalline powders of alkaline-earth hydroxyapatites, A10(PO4)6(OH)2 (A = Ca, Sr and Ba). J. Mater. Sci. 41, 1455–1458. doi:10.1007/s10853-006-7460-4
Pettersson, A., Åmand, L.-E., Steenari, B.-M., 2008a. Leaching of ashes from co-combustion of sewage sludge and wood—Part II: The mobility of metals during phosphorus extraction. Biomass Bioenerg. 32, 236–244. doi:10.1016/j.biombioe.2007.09.006
Pettersson, A., Åmand, L.-E., Steenari, B.-M., 2008b. Leaching of ashes from co-combustion of sewage sludge and wood—Part I: Recovery of phosphorus. Biomass Bioenerg. 32, 224–235. doi:10.1016/j.biombioe.2007.09.016
Peters, F., Schwarz K., Epple M., 2000. The structure of bone studied with synchrotron X-ray diffraction, X-ray absorption spectroscopy and thermal analysis. Thermochim. Acta 361(1-2): 131-138.
Petzet, S., Peplinski, B., Cornel, P., 2012. On wet chemical phosphorus recovery from sewage sludge ash by acidic or alkaline leaching and an optimized combination of both. Water Res. 46, 3769–3780. doi:10.1016/j.watres.2012.03.068
Ragauskas, A.J., 2006. The Path Forward for Biofuels and Biomaterials. Science. 311, 484–489. doi:10.1126/science.1114736
Rajendran, J., Gialanella S., Aswath P. B., 2013. XANES analysis of dried and calcined bones. Mat. Sci. Eng. C-Mater. 33(7): 3968-3979.
Ravel, B., Newville M., 2005. ATHENA, ARTEMIS, HEPHAESTUS: data analysis for X-ray absorption spectroscopy using IFEFFIT. J. Synchrotron Radiat. 12: 537-541.
Rittmann, B.E., Mayer, B., Westerhoff, P., Edwards, M., 2011. Capturing the lost phosphorus. Chemosphere 84, 846–853. doi:10.1016/j.chemosphere.2011.02.001
Saidur, R., Abdelaziz, E.A., Demirbas, A., Hossain, M.S., Mekhilef, S., 2011. A review on biomass as a fuel for boilers. Renew. Sustain. Energy Rev. 15, 2262–2289. doi:10.1016/j.rser.2011.02.015
Sattari, S.Z., Bouwman, A.F., Giller, K.E., van Ittersum, M.K., 2012. Residual soil phosphorus as the missing piece in the global phosphorus crisis puzzle. Proc. Natl. Acad. Sci. U. S. A. 109, 6348–53. doi:10.1073/pnas.1113675109
Simons, A., Solomon, D., Chibssa, W., Blalock, G., Lehmann, J., 2014. Filling the phosphorus fertilizer gap in developing countries. Nat. Geosci. 7, 3–3. doi:10.1038/ngeo2049
Stegemann, J.A., Côté, P.L., 1991. Acid Neutralization Capacity, Appendix B: Investigation of test methods for solidified waste evaluation—a cooperative program, Manuscript Series TS-15, Environment Canada Wastewater Technology Centre, Burlington, Ontario Canada.
Štulajterová, R., Medvecký, Ľ., 2008. Effect of calcium ions on transformation brushite to hydroxyapatite in aqueous solutions. Colloids Surfaces A Physicochem. Eng. Asp. 316, 104–109. doi:10.1016/j.colsurfa.2007.08.036

Sugiyama, S., Kitora, R., Kinoshita, H., Nakagawa, K., Katoh, M., Nakasaki, K., 2016. Recovery of Calcium Phosphates from Composted Chicken Manure. J. Chem. Eng. Japan 49, 224–228. doi:10.1252/jcej.15we111

Szögi, A.A., Vanotti, M.B., Hunt, P.G., 2015. Phosphorus recovery from pig manure solids prior to land application. J. Environ. Manage. 157, 1–7.

Tan, Z., Lagerkvist, A., 2011. Phosphorus recovery from the biomass ash: A review. Renew. Sustain. Energy Rev. 15, 3588–3602. doi:10.1016/j.rser.2011.05.016

Tayibi, H., Choura, M., López, F.A., Alguacil, F.J., López-Delgado, A., 2009. Environmental impact and management of phosphogypsum. J. Environ. Manage. 90, 2377–2386. doi:10.1016/j.jenvman.2009.03.007

Tilman, D., Fargione, J., Wolff, B., D'Antonio, C., Dobson, A., Howarth, R., Schindler, D., Schlesinger, W.H., Simberloff, D., Swackhamer, D., 2001. Forecasting agriculturally driven global environmental change. Science 292, 281–284. doi:10.1126/science.1057544

Tilman, D., Lehman, C., 1987. Human-caused environmental change : Impacts on plant diversity and evolution. Proc. Natl. Acad. Sci. U. S. A. 98, 5433–5440. doi:10.1073/pnas.091093198

United States Geological Survey, 2019. Phosphate Rock, Mineral Commodity Summaries, p. 122-123. Available from: https://prd-wret.s3-us-west-2.amazonaws.com/assets/palladium/production/atoms/files/mcs-2019-phosp.pdf [accessed 17/6/19].

Vassilev, S. V., Baxter, D., Andersen, L.K., Vassileva, C.G., 2013a. An overview of the composition and application of biomass ash. Part 2. Potential utilisation, technological and ecological advantages and challenges Fuel 105, 19–39. doi:10.1016/j.fuel.2012.10.001

Vassilev, S. V., Baxter, D., Andersen, L.K., Vassileva, C.G., 2013b. An overview of the composition and application of biomass ash. Part 1. Phase–mineral and chemical composition and classification. Fuel 105, 40–76. doi:10.1016/j.fuel.2012.09.041

Vassilev, S. V., Baxter, D., Andersen, L.K., Vassileva, C.G., Morgan, T.J., 2012. An overview of the organic and inorganic phase composition of biomass. Fuel 94, 1–33. doi:10.1016/j.fuel.2011.09.030

Vassilev, S. V., Baxter, D., Vassileva, C.G., 2013c. An overview of the behaviour of biomass during combustion: Part I. Phase-mineral transformations of organic and inorganic matter. Fuel 112, 391–449. doi:10.1016/j.fuel.2013.05.043

Wilfert, P., Kumar, P.S., Korving, L., Witkamp, G.J., Van Loosdrecht, M.C.M., 2015. The Relevance of Phosphorus and Iron Chemistry to the Recovery of Phosphorus from Wastewater: A Review. Environ. Sci. Technol. 49, 9400–9414. doi:10.1021/acs.est.5b00150

Williams, A.G., Leinonen, I., Kyriazakis, I., 2016. Environmental benefits of using turkey litter as a fuel instead of a fertiliser. J. Clean. Prod. 113, 167–175. doi:10.1016/j.jclepro.2015.11.044

Wu, S., Wang, L., Zhao, L., Zhang, P., El-shall, H., 2018. Recovery of rare earth elements from phosphate rock by hydrometallurgical processes – A critical review. Chem. Eng. J. 335, 774–800. doi:10.1016/j.cej.2017.10.143

Zhang, F.S., Yamasaki, S., Kimura, K., 2002. Waste ashes for use in agricultural production: II. Contents of minor and trace metals. Sci. Total Environ. 286, 111–118. doi:10.1016/S0048-9697(01)00968-8

Figure captions

Fig. 1 X-ray powder diffraction (XRD) (a), Fourier transform infrared spectra (FTIR, normalised) (b), Thermogravimetric (TG/DTG) (c), and P K-edge X-ray absorption near edge structure (XANES, normalised) (d) analyses of meat and bone meal (MBM) bottom ashes (BA) and air pollution control residue (APCr), and poultry litter co-combustion (PL) bottom ash and residues from leaching of the same residues at pH 5.1-6.8. The reference materials Morrocan apatite (carbonate apatite), brushite, and apatite (hydroxyapatite) were all analyzed by FTIR, TG/DTG, and XANES, but only the references most relevant to each figure were presented; XRD references were from the XRD pattern database (International Centre for Diffraction Data, ICDD).

Fig. 2 Concentration of available P in meat and bone meal (MBM) bottom ashes (BA) and air pollution control residue (APCr), and poultry litter co-combustion (PL) bottom ash and residues from leaching of the same residues at pH 5.1-6.8. Error bars represent the standard deviation of three replicates.

Fig. 3 Anion leaching from meat and bone meal (MBM) bottom ashes (BA) and air pollution control residue (APCr), and poultry litter co-combustion (PL) bottom ash in the Acid Neutralization Capacity test (circled points are those for which the leached residue was characterised).

Fig. 4 Major element leaching from meat and bone meal (MBM) bottom ashes (BA) and air pollution control residue (APCr), and poultry litter co-combustion (PL) bottom ash in the Acid Neutralization Capacity test (circled points are those for which the leached residue was characterised).

Fig. 5 P recovery (average of duplicates) from meat and bone meal (MBM) bottom ashes (BA) and air pollution control residue (APCr), and poultry litter co-combustion (PL) bottom ash using H_2SO_4 and HNO_3, (a) Acid consumption comparison between H_2SO_4 and HNO_3; (b) P recovery percentage using H_2SO_4. Leaching time 2 h; Solid/liquid ratio 0.1.

*Graphical Abstract

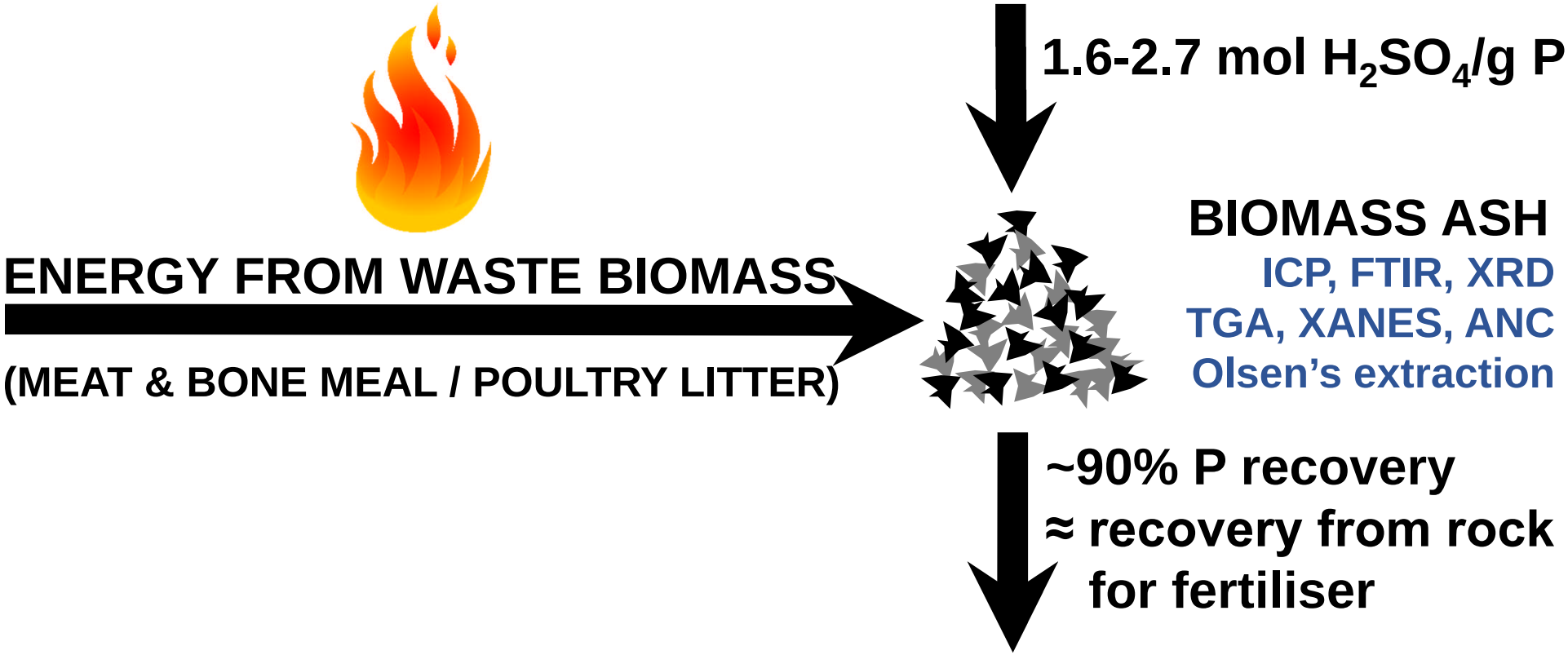

*Highlights (for review : 3 to 5 bullet points (maximum 85 characters including spaces per bullet point)

Characterisation of ashes from waste biomass power plants and phosphorus recovery

Lijian Leng, Anna A. Bogush, Amitava Roy, Julia A. Stegemann*

Highlights

- Meat and bone meal (MBM) and poultry litter (PL) biomass ashes were characterised
- P is mainly $Ca_5(PO_4)_3(OH)$ in MBM ashes and $KNaCa_2(PO_4)_2$ in PL ashes
- P recovery by acid dissolution seems feasible and promising
- Optimized acid consumption for ~90% P recovery is as low as 3.2-5.3 mol H^+/mol P

Characterisation of ashes from waste biomass power plants and phosphorus recovery

Lijian Leng [a], Anna A. Bogush [b], Amitava Roy [c], Julia A. Stegemann [b *]

[a] *School of Resources, Environmental & Chemical Engineering and Key Laboratory of Poyang Lake Environment and Resource Utilization, Ministry of Education, Nanchang University, Nanchang, 330031, China*

[b] *Centre for Resource Efficiency & the Environment, Department of Civil, Environmental & Geomatic Engineering, University College London, Chadwick Building, Gower Street, London WC1E 6BT, UK*

[c] *J. Bennett Johnston, Sr., Center for Advanced Microstructures & Devices, Louisiana State University, 6980 Jefferson Hwy, Baton Rouge, LA 70806, USA*

[*] *Corresponding author. Tel.: +44 (0)2076797370*

E-mail address: j.stegemann@ucl.ac.uk (J.A. Stegemann)

Abstract: Biowastes, such as meat and bone meal (MBM), and poultry litter (PL), are used as energy sources for industrial combustion in the UK. However, the biomass ashes remaining after combustion, which contain nutrients such as phosphorus, are landfilled rather than utilised. To promote their utilisation, biomass ashes from industries were characterised in terms of their elemental and mineral compositions, phosphorus extractability, and pH-dependent leachability. These ashes were highly alkaline (pH as high as 13), and rich in calcium and phosphorus. The P bio-availabilities in the ash evaluated by Olsen's extraction were low. Hydroxyapatite and potassium sodium calcium phosphate were identified by X-ray powder diffraction (XRD) as the major phases in the MBM and PL ashes, respectively. The leaching of P, Ca, and many other elements was pH dependent, with considerable increase in leaching below about pH 6. P recovery by acid dissolution (e.g., with H_2SO_4) seems feasible and promising; the optimized acid consumption for ~90% P recovery could be as low as 3.2-5.3 mol H^+/mol P.

Keywords: incineration; fertiliser; phosphorus recovery; acid neutralisation capacity; animal manure

1. Introduction

Thermal or biological processing of biomass produces heat, electricity, or liquid/gas/solid bioenergy with low net greenhouse gas emissions (Ragauskas, 2006). Wood and wood wastes, agricultural crops and their waste byproducts, animal wastes, wastes from food processing, aquatic plants, and algae are the most widely used biomass energy resources (Bogush et al., 2018; Demirbas, 2004; Huang and Yuan, 2015; Leng et al., 2018a, 2018b, 2016; Saidur et al., 2011). These biomass resources, which are currently often treated as organic wastes, can contribute significantly to the generation of renewable energy and reduction of greenhouse gas (GHG) emissions, reducing the dependency on fossil fuels (Ragauskas, 2006). The UK, for example, sets a target of 80% GHG emissions reduction over 1990 levels by 2050; the bioenergy industry contributes significantly to the achievement of these goals (Adams et al., 2011).

Consequently, recovery of energy from biomass by combustion or production of fuel, e.g., from straw, meat and bone meal, poultry litter, wood shavings, and horse bedding, is increasing in the UK, due to the mounting production of these wastes, their energy contents, and the environmental benefits of their utilisation (Oshita et al., 2016; Williams et al., 2016). However, management of ash has emerged to be one of the problems impeding the development of biomass combustion for energy (Niu et al., 2016). Since biomass ashes are rich in the nutrients phosphorus and potassium, they have been considered for use as a soil amendment on agricultural land. However, the low P availability, high alkalinity (e.g., pH 13 or higher), and heavy metal contents in these ashes may restrict their direct application (Niu et al., 2016; Vassilev et al., 2013a; Bogush et al., 2018). Environmental pollution from nutrient and contaminant leaching can occur, and result in negative effects on crops, soils and water, when

ashes are applied under soil and climatic conditions that increase environmental mobility of contaminants (Pettersson et al., 2008a; 2008b), or mobilise nutrients but do not favour their agronomic utilization, e.g., due to excessive application or an imbalance in the nutrient proportions (Bolan et al., 2010; Codling et al., 2002; Szögi et al., 2015; Williams et al., 2016). However, it is worth mentioning that environmental pollution by nutrients and contaminants has also been observed for soil fertilized with animal residues (e.g., pig slurry) directly (Cela et al., 2010; Gunkel-Grillon et al., 2015; Olson et al., 2010).

Meanwhile, the widespread global use of P fertiliser over the past century and increasing demand for P by agriculture threatens to deplete sources of P-bearing rock within the next century (Cordell et al., 2009; 2010; Mayer et al., 2016; Sattari et al., 2012; Tilman et al., 2001; Tilman and Lehman, 1987). Even ignoring rapidly increasing P demand, the estimated static lifetime of phosphorus reserves is only around 350 years (IFDC, 2010). Furthermore, the remaining reserves are highly geographically concentrated (Elser and Bennett, 2011), with around 71% located in Morocco and the Western Sahara (USGS, 2019). Therefore, sourcing P from the P consumption lifecycle and developing appropriate P recovery technology, especially in places with a scarcity of natural P-bearing rock such as the UK, is important to meet the increasing demand for this element (Cooper, 2014; Cordell et al., 2011; Mayer et al., 2016; Rittmann et al., 2011). Phosphorus recovery from animal residues (e.g., poultry litter, meat and bone meal) and sewage sludge, and their incineration ashes, is one of the most promising ways to increase the P resource security and secure future food production (Akinola, 2013; Bogush et al., 2018; Havukainen et al., 2016; Kleemann et al., 2015; Mayer et al., 2016; Tan and Lagerkvist, 2011). Cooper and Carliell-Marquet (2013) estimated that the P recovery potential from animal

manure produced in the UK could be higher than national net total P imports; in general, the P value of meat and bone meal/animal bone alone is likely of a similar order of magnitude to that of a country's phosphate fertiliser imports (Cooper and Carliell-Marquet, 2013; Simons et al., 2014).

Hence, recovery of P from biomass ashes to produce more effective and environmentally benign P fertilizer is of increasing interest for both research and practice. Animal manures and manure derivatives such as ash and char have been widely explored for P recovery, with measurement of varied recovery rates and acid demands because of differences between the sources (e.g., P concentration 4.0-139 g kg^{-1}) and process conditions (e.g., different acid types and loads, and solid/liquid ratios) (Table 1). For example, P recovery rates around 90% were obtained for animal manure char, but at acid loads in the region of 100 mol H^+/mol P recovered (Azuara et al., 2013; Heilmann et al., 2014). Lower acid loads (3-10 mol H^+/mol P recovered) were found effective for P recovery from manures and their ashes (Cohen, 2009; Kaikake et al., 2009; Kuligowski and Poulsen, 2010), which is similar to the recovery rates and acid loads for P recovery from sewage sludge ash (Petzet et al., 2012). In addition to P content and recovery conditions, P speciation in the different P-containing resources (wastes) also influences P recovery performance. Elemental, mineral and chemical compositions have been used to describe P speciation in these materials (Bogush et al., 2018; Vassilev et al., 2013a, 2013b, 2013c), but few studies have related these results to P recovery performance. Furthermore, little has been reported regarding meat and bone meal (MBM) and its derivatives (e.g., ash), despite the high P recovery potential from these materials.

The main objectives of this research were thus:

1) to characterise biomass ashes from combustion of MBM or co-combustion of

poultry litter (PL) in UK biomass power plants (https://biofuelwatch.org.uk/wp-content/maps/uk-biomass.html), and

2) to examine the potential and options for P recovery from these biomass ashes.

The bioavailability of P from biomass ashes and potential for its recovery from the biomass ashes depends on P speciation and matrix composition. The biomass ashes were therefore characterised by multiple techniques, including elemental analysis, thermogravimetric analysis (TGA), determination of crystalline phases by X-ray powder diffraction (XRD), characterization of functional groups by Fourier transform infrared spectroscopy (FTIR), and measurement of acid neutralization capacity (ANC) and pH-dependent P leachability, to understand the mechanisms responsible for control of P solubility. P K-edge X-ray absorption near edge spectroscopy (XANES) was used to examine the speciation of P in complex matrices without interference from irrelevant phases and irrespective of crystallinity.

2. Materials and methods

2.1 Materials

Five samples of biomass ash were collected from four different industrial-scale biomass power plants in the UK that use different biomass types as the energy source. The plants use moving grate incinerators with a combustion temperature of 850 ^{o}C, dry discharge of bottom ash, and dry scrubbing of the flue gas. MBM1-BA and MBM2-BA were bottom ashes collected from two different plants that combust MBM; MBM2-APCr was the fly ash from the second plant. PL1-BA and PL2-BA were both bottom ashes from different power plants that co-combust PL. The moisture contents of the biomass ashes were negligible (Bogush et al., 2018). The samples were ground to < 250 µm using a ball mill and then stored in air-tight containers before use.

Reference materials used in the mineralogical investigation included a Ward's

Science Apatite Research Mineral (www.wardsci.com; Catalogue No. 470026-560), a Moroccan apatite (carbonate apatite), and brushite ($CaHPO_4 \cdot 2H_2O$, 99.0%, Sigma-Aldrich).

2.2 Biomass ash elemental composition and bioavailability of P

The biomass ashes were subjected to total digestion using HNO_3: $HClO_4$: H_2O_2 (v, 30%) = 5:5:3, v/v) (Leng et al., 2014) before chemical analysis for the elements of interest (Section 2.7). Separate extracts for P analysis (Section 2.7) were prepared by digestion with potassium persulfate at 150^{o}C for 4.0 h.

Olsen's method has been widely used to evaluate the bioavailability of phosphorus (Olsen et al., 1954). The extraction was conducted in for all of the biomass samples and residues from leaching at mildly acidic pH (Section 2.5) by mixing 2.5 g ash with 50 mL 0.5 M of sodium bicarbonate (pH 8.5) and shaking for 30 min before separation of the extracts for analysis (Section 2.7).

2.3 Biomass ash mineralogy

The crystalline phases present in the biomass ashes and residues after leaching at mildly acidic pH (Section 2.5) were identified by XRD analysis on an XPERT-PRO diffractometer with an X-ray source of Cu K_α radiation at 40 KV and 30 mA. A scanning speed of 4 s per step and step size of 0.05° (2θ) were used in the scanning range of 5°–70° (2θ). The XRD data were analysed by using Jade software version 6.0 (Materials Data Inc., Livermore, USA).

Fourier transform infrared spectra (FTIR) of the biomass ashes, residues, and reference materials were obtained on a Thermo-Fischer Scientific Nicolet 670 spectrometer in the wavelength range of 400–4000 cm^{-1}.

Thermogravimetric analysis of the biomass ashes, residues, and reference materials was conducted by heating from room temperature to 1000 ^{o}C at a rate of 10 ^{o}C/min

under nitrogen atmosphere.

2.4 Phosphorus speciation

The speciation of P in the biomass ashes and residues after leaching at mild acidic pH (Section 2.5) was assessed by comparing their P K-edge X-ray absorption near edge structure (XANES) spectra with those of the reference materials. P K-edge measurements were made at the Low Energy X-ray Absorption Spectroscopy (Lexas) beamline of Louisiana State University's synchrotron research facility, the J. Bennett Johnston, Sr. Center for Advanced Microstructures and Devices (CAMD), USA. Lexas is a windowless beamline, i.e., with only a 13 µm think Katon™ window separating the ring from the experimental chamber. A University of Bonn-designed Lemonnier type monochromator with InSb 111 crystals was used in measurements. The measurements were made in fluorescence by diluting the sample as necessary with boron nitride to reduce self-absorption (Oxmann, 2014). A Ketek 150 mm^2 silicon drift detector was used for fluorescence measurements. The white line of reagent grade aluminum phosphate was used to calibrate the monochromator at 2152.8 eV. The parameters for the measurements were 2050 eV to 2110 eV with 5 eV steps, 2110 eV to 2142 eV with 0.5 eV steps, 2142 eV to 2160 eV with 0.1 eV steps, from 2160 to 2180 eV with 0.5 eV steps, and 2180 eV to 2250 eV with 1 eV steps. The integration time was from 1 to 5 seconds for adequate counting statistics. The spectra were analyzed with Athena in Demeter (Ravel and Newville, 2005).

2.5 pH-dependent leaching

The acid neutralization capacity (ANC) of the biomass ashes was measured to examine their pH responses to acid addition, and the consequent changes in the solubilities of their components of interest. This test involves adding increasing amounts of nitric acid to a series of 10 or more subsamples of the material under

investigation (Stegemann and Côté, 1991). A single series of 5.0 g subsamples was weighed out for each of the biomass ashes and mixed with 30 mL of nitric acid diluted with deionized water to a concentration from 0 to 3 N (up to 18 meq/g of biomass ash) HNO_3. After 48h of end-over-end mixing at 30 rpm, the samples were centrifuged, and the pH values and conductivities of all the supernatants were measured before separation of the leachates for analysis. The solid residues corresponding to leachates with mild acidic pH (6.2, 5.1, 5.9, 6.5, and 6.8 for MBM1-BA, MBM2-BA, MBM2-APCr, PL1-BA, and PL2-BA, respectively (Table S1) were also analysed by XRD (Section 2.3) FTIR (Section 2.3), XANES (Section 2.4), and Olsen's method (Section 2.2) after drying at 60 ^{o}C.

2.6 Acid extraction for phosphorus recovery

To further assess acid extractability of P from the biomass ashes, the effects of contact time (0-48 h), liquid/solid ratio (4-20 mL/g of ash), acid type (HNO_3 and H_2SO_4), and acid load (6-16 meq H^+/g ash) were investigated with the volume of the extraction liquid fixed at 30 mL. Experiments were conducted in duplicate. P recovery rate was defined as the percentage of P in the leachate as compared with that in the original ash.

2.7 Chemical analysis of extracts and leachates

Liquid samples from digestion, extraction, and wastewater treatment were filtered from the solids through 0.45 µm membrane filters; leachates for metal analysis were acidified to pH 2 before storage.

P in the filtered liquid samples was determined by colorimetry at 880 nm, by reaction with ammonium molybdate using ascorbic acid as the reducing agent (Murphy and Riley, 1962).

Metals, including Al, B, Bi, Ba, Ca, Co, Cr, Cu, Cd, Fe, K, Mg, Li, Mn, Na, Ni, Pb,

Sr, and Zn, and P in the extracts from total digestion of the biomass ashes and the ANC test leachates were determined by Inductively Coupled Plasma Optical Emission Spectroscopy (ICP-OES).

Anions in the ANC leachates, including F^-, Cl^-, Br^-, NO_2^-, NO_3^-, PO_4^{3-} and SO_4^{2-}, were analysed by a Dionex AQUION Ion Chromatography (IC) before acidification of the samples.

All chemical analyses were conducted in triplicate with reporting of mean values.

3. Results and discussion

3.1 Biomass ash elemental composition and bioavailability of P

The elemental compositions of the biomass ashes in Table 2 are typical for ashes from animal residue incineration (Bogush et al., 2018; Oshita et al., 2016; Vassilev et al., 2012; Zhang et al., 2002). Apart from P, the major elements are Al, Fe, K, Mg, Mn, and Na, with Ca as the most abundant element comprising 16-32% of the total ash.

The P concentrations of these ashes range from 8.3-13%, which is comparable to that of some natural phosphorus rocks [e.g., 30–40% P_2O_5; 13–17.5% P (Desmidt et al., 2015; Elouear et al., 2008)]. However, Fig. 2 shows that the contents of bioavailable P in the ashes are less than 800 mg P/kg ash, corresponding to <0.7% of the total P.

The contents of K and, especially, Mg, in the PL ashes are higher than those of the MBM ashes. Some differences between the compositions of ashes from different MBM incineration plants can also be observed, e.g., MBM1-BA has higher contents of Ca and P, and lower contents of K and Na compared to MBM2-BA, showing the effects of variations in the original MBM materials. Minor elements such as B, Zn, Sr, Ba, and Cu are in the range of 100-1100 mg/kg, while trace elements such as Bi, Cd,

Cr, Co, Li, Ni, and Pb are <100 mg/kg.

3.2 Biomass ash mineralogy

Fig. 1(a) shows that the dominant phase identified in the MBM ashes by XRD is hydroxyapatite (HAP), which is consistent with the high contents of Ca and P. Hydroxyapatite, with some carbonation, is the principal mineral in bone (e.g., Elliott, 2002), and increases in crystallinity with heating. Both β-tricalcium phosphate [β-$Ca_3(PO_4)_2$, β-TCP] and HAP were identified by XRD as the major phases in either dried or calcined bones (Brod et al., 2015; Rajendran et al., 2013). XRD identified potassium sodium calcium phosphate [$KNaCa_2(PO_4)_2$] as the main phase in the PL ashes. This phase is also identified as the major mineral phase after combustion of P and Ca-bearing biomass at a temperature of 815 ^oC (Kongsomart et al., 2016). The solubility of apatite varies significantly depending on its content of other anions (e.g., CO_3^{2-}, Cl^- or F^-) (Magalhães and Williams, 2007), but $Ca_5(PO_4)_3(OH)$, which has K_{sp} = 3.98×10^{-59} (Chow, 2001; Delvasto et al., 2006) might be expected to have low bioavailability, as was observed for the biomass ashes (Section 3.1). No data about bioavailability was found for $KNaCa_2(PO_4)_2$.

A comparison of the Moroccan apatite FTIR spectrum with those of the ashes [Fig. 1(b)] shows that all are dominated by the ca. 1030 cm^{-1} (anti-symmetric stretch Υ_3) band, with the Υ_1 (ca. 960 cm^{-1}) and symmetric stretch Υ_4 bands (F_2 bend 650-525 cm^{-1}) also being conspicuous; the resemblance to the reference material is most obvious for MBM1-BA and MBM2-APCr. However, all phosphate bands show some shift, indicating variations in composition, e.g., substitution of CO_3^{2-} in the crystal structure. The CO_3^{2-} ion can be found in the channels (A type) of the hexagonal crystal structure of apatite, or substitutes for the phosphate ion (B type). With B type carbonate apatite, there is a doublet around 1430 cm^{-1} (Fleet, 2009), as seen in the

Moroccan apatite. PL1-BA thus seems to contain carbonate apatite whereas the other ashes showed only hydroxyapatite. The OH^- peak at 3420 cm^{-1} in all FTIR spectra is quite weak, but the derivative thermogravimetric (DTG) curves [Fig. 1(c)] show that all ashes have mass loss peaks in the region 200 °C to 400 °C. A comparison with apatite standards used in this study (not shown) and data from the literature suggests this peak is from the OH in the apatite in the ashes. The DTG curves also have doublets, which vary in strength depending on the biomass ash, in the region 600°C to 800°C, one of which is likely from the carbonate in the apatite structure, whereas the other one is calcium carbonate (Peters et al., 2000).

Previous studies have also found hydroxyapatite and $KNaCa_2(PO_4)_2$ (Bogush et al., 2018; Coutand et al., 2008; Komiyama et al., 2013; Oshita et al., 2016; Sugiyama et al., 2016), but also other minerals, e.g., $Ca_3(PO_4)_2$ in ashes from MBM or animal manure combustion (Coutand et al., 2008; Sugiyama et al., 2016) and $Ca_9MgK(PO_4)_7$ in manure ashes (Komiyama et al., 2013; Oshita et al., 2016).

XRD also showed portlandite [$Ca(OH)_2$] in the MBM ashes, which is corroborated by the 3643 cm^{-1} FTIR band, suggestive of OH^- in $Ca(OH)_2$ for all ashes but PL1-BA. The single similar carbonate band around 1430 cm^{-1} (Υ_3) in the FTIR spectra of all ashes except PL1-BA is typical of calcite, corresponding to calcite ($CaCO_3$) peaks in the XRD patterns except PL ashes.

XRD indicates sulphate to be present as calcium sulphate ($CaSO_4$) in all MBM ashes (Table 3), and arcanite (K_2SO_4) in the MBM2 and PL ashes. The FTIR spectra of MBM2-BA and PL2-BA are unlike those of the other ashes due to higher amounts of arcanite, which presents as peaks at 618 cm^{-1}, 1100 cm^{-1} and 1197 cm^{-1}. Sulfate breakdown may be responsible for the peak observed in the DTG at 931°C (MBM2-APCr).

XRD also shows quartz (SiO_2) in the PL ashes and MBM1-BA, and abundant halite (NaCl) in MBM2-APCr and MBM2-BA.

3.3 Phosphorus speciation

Fig. 1(d) shows the phosphorus K-edge XANES spectra of the samples along with that of the Ward's Science apatite. The white line position (A) of the latter is 2151.84 eV, while that of the ash samples ranges from 2151.67 eV to 2151.85 eV. The phosphate white line is from resonance between 1s and higher energy t_2* orbitals, while the peak around 2168 eV is from the P-O bond. The location and intensity of the C and D maxima depend on the composition and crystallinity of the phosphate phases (Ingall et al., 2011). These ashes thus have different phosphate compositions. Linear combination fitting of the spectrum of the MBM1-BA ash shows it to be principally composed of apatite, but the fit of apatite was not as good for the other ashes. The inflection of the shoulder at ~2155 eV correlates with the Ca/P ratio of the structure (Franke and Hormes, 1995); consequently, the PL ashes, which are indicated by XRD to contain $KNaCa_2(PO_4)_2$, appear to have a lower Ca/P ratio than the MBM ashes, in which $Ca_5(PO_4)_3(OH)$ was identified as the main P-bearing mineral.

There are some contradictions when comparing mineralogy results obtained from different analytical techniques. The variance between mineralogical analyses can be expected when applying different techniques to very small samples, particularly for complex materials such as these. Mineral phases identified by XRD were used in the following discussions unless specified otherwise.

3.4 pH dependent leaching and characterisation of the leached residues

The leachate pH values resulting from the discrete acid loading (on the secondary ordinate in Figs. 3 and 4) suggest a small, near vertical, plateau corresponding to neutralisation of the abundant $Ca(OH)_2$ in the MBM ash at pH ~12; this plateau is

311 absent for the PL ashes, which contain little $Ca(OH)_2$ (section 3.2).

312 A second pH plateau at ~7 may be attributable to several different phenomena.
313 Dissolution of the small component of calcite in the ashes, which will yield a pH
314 lower than that of 8.3 expected in equilibrium with the atmosphere since the leaching
315 tubes are sealed, likely contributes to this plateau. For the MBM ashes, the plateau
316 also reflects dissolution of $Ca_5(PO_4)_3(OH)$, which has an equilibrium pH of ~7.5
317 (based on the K_{sp} noted above). Perhaps most importantly, a phosphate buffer system
318 will result from dissolution of the apatite, and, especially, $KNaCa_2(PO_4)_2$. The second
319 plateau is more apparent for the PL ashes, which had an acid neutralization capacity
320 of 9-10 meq H^+/g to pH 4, whereas it was only 5-6 H^+ meq/g for the MBM ashes.
321 There is a third pH plateau, below pH 4.

322 Fig. 3 shows that sulfate, released at high pH by dissolution of K_2SO_4, drops in
323 concentration below pH 8, likely due to precipitation of gypsum ($CaSO_4 \cdot 2H_2O$; K_{sp} =
324 2.62×10^{-5}; Harouaka et al., 2014), as Ca enters solution from calcite and the
325 phosphate minerals (Fig. 4). Since there is little K_2SO_4 to dissolve from MBM1-BA,
326 Ca is not precipitated and its leached concentration is therefore higher than for the
327 other ashes.

328 Fig. 3 shows constant concentrations of chloride regardless of pH for each
329 biomass ash, consistent with the presence of NaCl identified by XRD. Na and K are
330 also initially released from NaCl and K_2SO_4, but their concentrations rise slightly as
331 the pH falls in the MBM ash leachates, and increase dramatically below pH 8 in the
332 PL ash leachates. P (Fig. 4, and phosphate, Fig. 3) concentrations are seen to be low
333 above pH ~4, and then increase as the phosphate minerals dissolve with further acid
334 addition. Release of Na and K with P from dissolution of the $KNaCa_2(PO_4)_2$ in the PL
335 ashes would be expected, but the increases in their concentrations before the

concentration of P starts to rise suggest that the dissolution of $KNaCa_2(PO_4)_2$ is incongruent, with selective loss of K and Na, or that this mineral dissolves and reprecipitates, e.g., as brushite ($CaHPO_4 \cdot 2H_2O$) (Johnsson and Nancollas, 1992).

Mg, Ba and Sr (Fig. S1) seem to be mainly released in association with the pH~7 plateau. They may substitute for Ca in calcite or phosphate minerals and are released when those dissolve. Cu and Zn form phosphates of low solubility and are mainly released below pH 4; the leaching rates of these elements were undetectable or at very low level at pH 8-12 from MBM1-BA (Fig. S1), because of the relatively low total contents of minor elements in this ash (Table 2). The concentrations of Fe were almost undetectable, and those of Al were negligible, in the leachates from the MBM ashes and PL2-BA. Iron oxides have low solubility, and it is possible that $Fe_3(PO_4)_2 \cdot 8H_2O/FePO_4$, $AlPO_4$, $Pb_5(PO_4)_3(OH)/Pb_3(PO_4)_2$, and $Zn_3(PO_4)_2$, which have low solubility, may exist in the original ashes or were formed as secondary precipitates during the test (Deydier et al., 2003; Parhi et al., 2006; Wilfert et al., 2015).

XRD of the residues in Fig. 1(a) from leaching at mildly acidic pH (5.1-6.8; Section 2.5) shows precipitation of $CaHPO_4 \cdot 2H_2O$ [$K_{sp} = 2.57 \times 10^{-7}$; (Chow, 2001)], which forms under acidic conditions (Johnsson and Nancollas, 1992). Dorozhkin's dissolution mechanism for hydroxyapatite (Eqs. 1–3) demonstrates that $Ca_5(PO_4)_3(OH)$ would produce $Ca_3(PO_4)_2$ ($K_{sp} = 3.16 \times 10^{-26}$ for α-$Ca_3(PO_4)_2$ and $K_{sp} = 1.26 \times 10^{-29}$ for β-$Ca_3(PO_4)_2$ (Chow, 2001)) at the first stage and then addition of additional acid would yield metastable $CaHPO_4$, and finally the dissolution of $CaHPO_4$ (Dorozhkin, 2012; 1997). Brushite solubility can markedly rise with a decrease in pH from 6 to 3 (Kuz'mina et al., 2013) and at lower pH it dissolves linearly (Figs. 3 and 4).

$$2Ca_5(PO_4)_3(OH) + 2H^+ \rightarrow 3Ca_3(PO_4)_2 + Ca^{2+} + 2H_2O \quad (1)$$

$$Ca_3(PO_4)_2 + 2H^+ \rightarrow 2CaHPO_4 + Ca^{2+} \quad (2)$$

$$CaHPO_4 + H^+ \rightarrow H_2PO_4^- + Ca^{2+} \quad (3)$$

The presence of $CaHPO_4 \cdot 2H_2O$ in the residues after leaching at mildly acidic pH (pH 5.1-6.8) was verified by multiple techniques. Fig. 1(a) shows that it dominates the XRD patterns of the leached residues, while the peak intensities for $Ca_5(PO_4)_3(OH)$ in MBM ashes are reduced and $KNaCa_2(PO_4)_2$ in PL ashes have almost disappeared. The prominent peak around 1650 cm^{-1} found in the FTIR spectra of all the leached residues as seen in [Fig. 1 (b)] corresponds to the molecular H_2O peak from $CaHPO_4 \cdot 2H_2O$ at 1645.48 cm^{-1}. The precipitation of $CaHPO_4 \cdot 2H_2O$ is also evident in the DTG traces for the leached residues of all the ashes as a peak at ~183°C [Fig. 1 (c)], with the amount ranging from 21.6-24.2%. Finally, the P K-edge XANES spectra [Fig. 1(d)] confirm that different phosphate phases are present in the leached residues than the original ashes, although fitting to estimate the exact P composition is difficult as several phosphate phases are present. Although $CaHPO_4 \cdot 2H_2O$ ($K_{sp} = 2.57 \times 10^{-7}$) in the residues is more soluble than $Ca_5(PO_4)_3(OH)$ ($K_{sp} = 3.98 \times 10^{-59}$), the bioavailable P in the solid residues separated from the mildly acidic leachates remained low at <1400 mg P/kg ash (Fig. 2). It is noteworthy that $CaHPO_4 \cdot 2H_2O$ can transform back to $Ca_5(PO_4)_3(OH)$ or $Ca_3(PO_4)_2$ in an alkaline and calcium-rich environment (Štulajterová and Medvecký, 2008).

During leaching, the water-soluble NaCl, K_2SO_4, and acid-soluble calcite and $Ca(OH)_2$ were not found in the leached residues, as shown in Fig. 1(a), but gypsum ($CaSO_4 \cdot 2H_2O$) and SiO_2 remained, as they are acid-insensitive over the pH range studied. The absence of the 618 cm^{-1} and 1195 cm^{-1} bands in the FTIR spectra of the leached residues [Fig. 1(b)] indicate the dissolution of the sulfate phases. The 713 cm^{-}

[1] carbonate band from calcite is very weak to non-existent in the residues [Fig. 1(b)]. In the thermogravimetric analysis of the leached residues, all the mass loss occurred by 600°C, and the absence of a calcite peak [Fig. 1(c)] reflect complete dissolution of calcite at the lower pH.

To summarize, NaCl and K_2SO_4 present in ashes dissolved readily with water leaching. Other chemical components dissolved with decreasing pH or increasing acid addition. Alkaline $CaCO_3$ and $Ca(OH)_2$ were neutralized at the first plateau and followed by the dissolution of $Ca_5(PO_4)_3(OH)$ and $KNaCa_2(PO_4)_2$ to produce $CaHPO_4 \cdot 2H_2O$ at pH~7, which continued to dissolve with releasing of P to the leachate from pH ~4. Mg, Ba and Sr mainly released in association with the pH~7 plateau while the release of Fe, Al, Zn, and Cu became evident at pH~4.

3.5 Phosphorus recovery from biomass ash

P release in the ANC test can be used to estimate the P recovery potential from the biomass ashes studied. Phosphorus recovery was found to be linearly dependent on the leachate pH below pH~4, attaining 40-50% at pH~3, and ~100% P recovery at pH~1 [Fig. S2(a)]. Determination of the acid consumption per unit of P recovered [Fig. S2(b)] is essential to assess the economic feasibility of the recovery process, and ranged from 9-14 meq H^+/g ash, assuming that the other ashes follow the trend established to 100% recovery for PL1-BA.

Investigation of the contact time showed that P recovery reached 75-95% of its highest value within several minutes [Fig. S3(a)], but the pH needed several hours to reach steady state [Fig. S3(b)]. This implies that P could be recovered promptly before surplus acid is consumed by the solid ash residue.

Solid/liquid (S/L) ratio also plays a significant role in P recovery; less acid was consumed per unit of P recovered at lower S/L ratios because of more efficient mixing

411 (Fig. S4). For example, results show that 10-20% less acid will be needed at S/L ratio
412 of 0.05, than at a S/L of 0.1, which is the ratio that has been widely used for P
413 dissolution from biomass ashes (Oshita et al., 2016; Sugiyama et al., 2016).
414 Unfortunately, a lower S/L ratio also produces a larger amount of leachate with a
415 lower P concentration, which could make the recycling of P and the subsequent
416 wastewater treatment much more difficult.

417 HNO_3 and H_2SO_4 were therefore applied at S/L 0.1, with a contact time of 2h, to
418 assess the influence of the acid type on P recovery and acid consumption. H_2SO_4
419 seems to be more efficient for P leaching from these biomass ashes compared with
420 HNO_3 particularly at lower acid load (Fig. 5). During the H_2SO_4 process, the
421 precipitation of gypsum promotes the dissolution of apatite, and facilitates the
422 separation of the product. By comparison, separation of dissolved $Ca(NO_3)_2$ formed
423 during HNO_3 leaching is difficult. At H_2SO_4 load of 14 meq H^+/g ash, the acid
424 consumption is in the range of 3.2-5.3 mol H^+/mol P (Fig. 5), which is comparable
425 with those reported in previous studies when animal manures or their derivatives (e.g.,
426 ashes) (Table 1) or sewage sludge ashes (Petzet et al., 2012) were used for P recovery.
427 Meanwhile, P recovery of ~90% or higher was achieved at this acid load.

428 *3.6 Economic considerations*

429 In the phosphorus industry, phosphoric acid is the basic starting raw material for
430 production, which is normally produced from phosphate rock. The wet process is the
431 most commonly used phosphoric acid production process, in which H_2SO_4 dissolves
432 $Ca_5(PO_4)_3(F, Cl, OH)$, followed with purification and condensation to produce
433 phosphoric acid (H_3PO_4) and byproduct phosphogypsum (Tayibi et al., 2009).
434 $Ca_5(PO_4)_3F$ is the dominant component of natural phosphate rock and its dissolution
435 mechanisms during wet-process phosphoric acid production can be described by Eqs.

4-7 (Dorozhkin, 1996), which are similar to those for $Ca_5(PO_4)_3(OH)$ (Eqs. 1-3). The overall reaction can be described by Eq. 8 (Wu et al., 2018).

$$2Ca_5(PO_4)_3(F, OH) + 2H^+ \rightarrow 3Ca_3(PO_4)_2 + Ca^{2+} + 2HF, H_2O \quad (4)$$

$$Ca_3(PO_4)_2 + 2H^+ \rightarrow 2CaHPO_4 + Ca^{2+} \quad (5)$$

$$CaHPO_4 + H^+ \rightarrow H_2PO_4^- + Ca^{2+} \quad (6)$$

$$H_2PO_4^- + H^+ \rightarrow H_3PO_4 \quad (7)$$

$$Ca_{10}(PO_4)_6(F, OH)_2 + 10H_2SO_4 + nH_2O \rightarrow 10CaSO_4 \cdot nH_2O + 6H_3PO_4 + 2HF, H_2O \quad (8)$$

The theoretical acid consumption for the wet-process phosphoric acid production is 3.3 mol H^+/mol P or 1.67 mol H_2SO_4/mol H_3PO_4. If the final product is $H_2PO_4^-$, the consumption drops to 2.3 mol H^+/mol P, which is the lowest acid addition needed to dissolve all P into the aqueous phase. However, the processes described by Eqs. 6 and 7 proceed at the same time; thus, the lowest theoretical acid consumption for P dissolution from $Ca_5(PO_4)_3(F, OH)$ would be 2.3-3.3 mol H^+/mol P. Considering the presence of minerals such as $CaCO_3$, $MgCO_3$, CaO, and MgO in natural phosphate rock, the consumption would be >2.3-3.3 mol H^+/mol P depending on the content of acid-consuming components, which is comparable to that of dissolution of MBM ashes (3.2-4.2 mol H^+/mol P). Furthermore, the dissolution of MBM ashes (composed of $Ca_5(PO_4)_3(OH)$) would not be complicated by the presence of fluorine, which is abundant in phosphate rock. Therefore, P recovery from MBM ashes by direct acid dissolution seems very promising and worth further investigation.

4. Conclusions

Hydroxyapatite [$Ca_5(PO_4)_3(OH)$] and potassium sodium calcium phosphate [$KNaCa_2(PO_4)_2$] seem to be the main mineral phases in the MBM and PL ashes, respectively, with low bioavailability of P. Phosphate leaching is pH dependent and

significant recovery was experienced at pH <4. Major heavy metals such as Cu and Zn demonstrated similar leaching behavior as P. A substantial proportion of the P remaining in the solid residues after acid leaching was transformed to brushite, but its bioavailability increased only slightly.

It appears that secondary P, for industrial production of fertilizer or other chemicals, could be recovered from MBM and PL ashes by acid dissolution (particularly by H_2SO_4), with acid consumption as low as 3.2-5.3 mol H^+/mol P and up to 90% P recovery. Particularly, the consumption when recovering P from MBM (3.2-4.2 mol H^+/mol P) is close to that required for P recovery from natural phosphate rock.

Acknowledgment

The research was financially supported by the British Council (Newton Fund) and the China Scholarship Council [File No. 201503780024]. The authors wish to thank Dr. Judith Zhou for helping with the IC analysis, Catherine Unsworth for running the ICP-OES analysis, and Dr. Shi Shi for carrying out the XRD analysis. We also gratefully acknowledge the biomass fuel plants, who chose to be anonymous, for providing the ash samples.

References

Adams, P.W., Hammond, G.P., McManus, M.C., Mezzullo, W.G., 2011. Barriers to and drivers for UK bioenergy development. Renew. Sustain. Energy Rev. 15, 1217–1227. doi:10.1016/j.rser.2010.09.039

Akinola, O., 2013. Overview of Phosphorus Recovery and Recycling From Selected Waste Streams - Protecting Phosphorus as a Resource. Imperial College London.

Azuara, M., Kersten, S.R.A., Kootstra, A.M.J., 2013. Recycling phosphorus by fast pyrolysis of pig manure: Concentration and extraction of phosphorus combined with formation of value-added pyrolysis products. Biomass Bioenerg. 49, 171–180. doi:10.1016/j.biombioe.2012.12.010

Bogush, A.A., Stegemann, J.A., Williams, R., Wood, I.G., 2018. Element speciation in UK biomass power plant residues based on composition, mineralogy, microstructure and leaching. Fuel 211, 712–725. doi:10.1016/j.fuel.2017.09.103

Bolan, N.S., Szogi, A.A., Chuasavathi, T., Seshadri, B., Rothrock, M.J., Panneerselvam, P., 2010. Uses and management of poultry litter. Worlds. Poult. Sci. J. 66, 673–698. doi:10.1017/S0043933910000656

Brod, E., Øgaard, A.F., Hansen, E., Wragg, D., Haraldsen, T.K., Krogstad, T., 2015. Waste products as alternative phosphorus fertilisers part I: inorganic P species affect fertilisation effects depending on soil pH. Nutr. Cycl. Agroecosystems 103, 167–185. doi:10.1007/s10705-015-9734-1

Cela, S., Berenguer, P., Santiveri, F., Lloveras, J., 2010. Potential phosphorus, potassium, and magnesium surpluses in an irrigated maize monoculture fertilized with Pig slurry. Agron. J. 102, 96–102. doi:10.2134/agronj2009.0139

Chow, L.C., 2001. Solubility of Calcium Phosphates. Octacalcium Phosphate l, 94–111. doi:10.1159/000061650

Cohen, Y., 2009. Phosphorus dissolution from ash of incinerated sewage sludge and animal carcasses using sulphuric acid. Environ. Technol. 30, 1215–1226. doi:10.1080/09593330903213879

Cooper, J., 2014. Managing phosphorus in the UK water industry to increase national resource security. The University of Birmingham.

Cooper, J., Carliell-Marquet, C., 2013. A substance flow analysis of phosphorus in the UK food production and consumption system. Resour. Conserv. Recycl. 74, 82–100. doi:10.1016/j.resconrec.2013.03.001

Cordell, D., 2010. The story of phosphorus: Sustainability implications of global phosphorus scarcity for food security. Linköping University.

Cordell, D., Drangert, J.O., White, S., 2009. The story of phosphorus: Global food security and food for thought. Glob. Environ. Chang. doi:10.1016/j.gloenvcha.2008.10.009

Cordell, D., Rosemarin, A., Schroder, J.J., Smit, A.L., 2011. Towards global phosphorus security: A systems framework for phosphorus recovery and reuse options. Chemosphere 84, 747–758. doi:10.1016/j.chemosphere.2011.02.032

Coutand, M., Cyr, M., Deydier, E., Guilet, R., Clastres, P., 2008. Characteristics of industrial and laboratory meat and bone meal ashes and their potential applications. J. Hazard. Mater. 150, 522–532. doi:10.1016/j.jhazmat.2007.04.133

Delvasto, P., Valverde, A., Ballester, A., Igual, J.M., Munoz, J.A., Gonzalez, F., Blazquez, M.L., Garcıa, C., 2006. Characterization of brushite as a re-crystallization product formed during bacterial solubilization of hydroxyapatite in batch cultures. Soil Biol. Biochem. 38, 2645–2654. doi:10.1016/j.soilbio.2006.03.020

Demirbas, A., 2004. Combustion characteristics of different biomass fuels. Prog. Energy Combust. Sci. 30, 219–230. doi:10.1016/j.pecs.2003.10.004

Desmidt, E., Ghyselbrecht, K., Zhang, Y., Pinoy, L., Van der Bruggen, B., Verstraete, W., Rabaey, K., Meesschaert, B., 2015. Global Phosphorus Scarcity and Full-Scale P-Recovery Techniques: A Review. Crit. Rev. Environ. Sci. Technol. 45, 336–384. doi:10.1080/10643389.2013.866531

Deydier, E., Guilet, R., Sharrock, P., 2003. Beneficial use of meat and bone meal combustion residue: “An efficient low cost material to remove lead from aqueous effluent.” J. Hazard. Mater. 101, 55–64. doi:10.1016/S0304-3894(03)00137-7

Dorozhkin, S. V, 2012. Dissolution mechanism of calcium apatites in acids: A review of literature. World J. Methodol. 2, 1–17. doi:10.5662/wjm.v2.i1.1

Dorozhkin, S. V, 1997. Surface Reactions of Apatite Dissolution. J. Colloid Interface Sci. 191, 489–497. doi:10.1006/jcis.1997.4942

Dorozhkin, S. V, 1996. Fundamentals of the Wet-Process Phosphoric Acid Production . 1 . Kinetics and Mechanism of the Phosphate Rock Dissolution. Ind. Eng. Chem. Res. 35, 4328–4335. doi:10.1021/ie960092u

Ekpo, U., Ross, A.B., Camargo-Valero, M.A., Fletcher, L.A., 2016. Influence of pH on hydrothermal treatment of swine manure: Impact on extraction of nitrogen and phosphorus in process water. Bioresour. Technol. 214, 637–644.

Elouear, Z., Bouzid, J., Boujelben, N., Feki, M., Jamoussi, F., Montiel, A., 2008. Heavy metal removal from aqueous solutions by activated phosphate rock. J. Hazard. Mater. 156, 412–420. doi:10.1016/j.jhazmat.2007.12.036

Elser, J., Bennett, E., 2011. A broken biogeochemical cycle. Nature 478, 29–31. doi:10.1038/478029a

Elliott, J. C., 2002. Calcium Phosphate Biominerals. Rev. Mineral. Geochem. 48(1): 427-453.

Fleet, M. E., 2009. Infrared spectra of carbonate apatites: ν2-Region bands. Biomaterials 30(8): 1473-1481.

Franke, R., Hormes, J., 1995. The P K-near edge absorption spectra of phosphates. Phys. B Phys. Condens. Matter 216, 85–95. doi:10.1016/0921-4526(95)00446-7

Grzmil, B., Wronkowski, J., 2006. Removal of phosphates and fluorides from industrial wastewater. Desalination 189, 261–268. doi:10.1016/j.desal.2005.07.008

Gunkel-Grillon, P., Roth, E., Laporte-Magoni, C., Le Mestre, M., 2015. Effects of long term raw pig slurry inputs on nutrient and metal contamination of tropical volcanogenic soils, Uvéa Island (South Pacific). Sci. Total Environ. 533, 339–46. doi:10.1016/j.scitotenv.2015.06.110

Harouaka, K., Eisenhauer, A., Fantle, M.S., 2014. Experimental investigation of Ca isotopic fractionation during abiotic gypsum precipitation. Geochim. Cosmochim. Acta 129, 157–176. doi:10.1016/j.gca.2013.12.004

Havukainen, J., Nguyen, M.T., Hermann, L., Horttanainen, M., Mikkilä, M., Deviatkin, I., Linnanen, L., 2016. Potential of phosphorus recovery from sewage sludge and manure ash by thermochemical treatment. Waste Manag. 49, 221–229. doi:10.1016/j.wasman.2016.01.020

He, Z., Pagliari, P.H., Waldrip, H.M., 2016. Applied and Environmental Chemistry of Animal Manure: A Review. Pedosphere 26, 779–816. doi:10.1016/S1002-0160(15)60087-X

Heilmann, S.M., Molde, J.S., Timler, J.G., Wood, B.M., Mikula, A.L., Vozhdayev, G. V, Colosky, E.C., Spokas, K. a, Valentas, K.J., 2014. Phosphorus Reclamation through Hydrothermal Carbonization of Animal Manures. Environ. Sci. Technol. doi:10.1021/es501872k

Huang, H., Yuan, X., 2015. Recent progress in the direct liquefaction of typical biomass. Prog. Energy Combust. Sci. 49, 59–80. doi:10.1016/j.pecs.2015.01.003

IFDC, 2010. World Phosphate Rock Reserves and Resources. International Fertilizer Development Centre.

Ingall, E. D., Brandes J. A., Diaz J. M., de Jonge M. D., Paterson D., McNulty I., Elliott W.C., Northrup P., 2011. Phosphorus K-edge XANES spectroscopy of mineral standards. J. Synchrotron Radiat 18: 189-197.

Johnsson, M.S.-A., Nancollas, G.H., 1992. The Role of Brushite and Octacalcium Phosphate in Apatite Formation. Crit. Rev. Oral Biol. Med. 3, 61–82. doi:10.1177/10454411920030010601

Kaikake, K., Sekito, T., Dote, Y., 2009. Phosphate recovery from phosphorus-rich solution obtained from chicken manure incineration ash. Waste Manag. 29,

1084–1088. doi:10.1016/j.wasman.2008.09.008
Kleemann, R., Chenoweth, J., Clift, R., Morse, S., Pearce, P., Saroj, D., 2015. Evaluation of local and national effects of recovering phosphorus at wastewater treatment plants: Lessons learned from the UK. Resour. Conserv. Recycl. 105, 347–359. doi:10.1016/j.resconrec.2015.09.007
Komiyama, T., Kobayashi, A., Yahagi, M., 2013. The chemical characteristics of ashes from cattle, swine and poultry manure. J. Mater. Cycles Waste Manag. 15, 106–110. doi:10.1007/s10163-012-0089-2
Kongsomart, B., Kannari, N., Takarada, T., 2016. Catalytic Effects of Biomass-Derived Ash on Loy Yang Brown Coal Gasification. Int. J. Biomass Renewables 5, 12–22.
Kuligowski, K., Poulsen, T.G., 2010. Phosphorus and zinc dissolution from thermally gasified piggery waste ash using sulphuric acid. Bioresour. Technol. 101, 5123–5130. doi:10.1016/j.biortech.2010.01.143
Kuz'mina, M.A., Zhuravlev, S. V., Frank-Kamenetskaya, O. V., 2013. The effect of medium chemistry on the solubility and morphology of brushite crystals. Geol. Ore Depos. 55, 692–697. doi:10.1134/S1075701513080072
Leng, L., Li, J., Wen, Z., Zhou, W., 2018a. Use of microalgae to recycle nutrients in aqueous phase derived from hydrothermal liquefaction process. Bioresour. Technol. 256, 529–542. doi:10.1016/j.biortech.2018.01.121
Leng, L., Li, J., Yuan, X., Li, J., Han, P., Hong, Y., Wei, F., Zhou, W., 2018b. Beneficial synergistic effect on bio-oil production from co-liquefaction of sewage sludge and lignocellulosic biomass. Bioresour. Technol. 251, 49–56. doi:10.1016/j.biortech.2017.12.018
Leng, L., Yuan, X., Huang, H., Jiang, H., Chen, X., Zeng, G., 2014. The migration and transformation behavior of heavy metals during the liquefaction process of sewage sludge. Bioresour. Technol. 167, 144–150. doi:10.1016/j.biortech.2014.05.119
Leng, L., Yuan, X., Shao, J., Huang, H., Wang, H., Li, H., Chen, X., Zeng, G., 2016. Study on demetalization of sewage sludge by sequential extraction before liquefaction for the production of cleaner bio-oil and bio-char. Bioresour. Technol. 200, 320–327. doi:10.1016/j.biortech.2015.10.040
Magalhães, M.C.F., Williams, P.A., 2007. Apatite Group Minerals Solubility and Environmental Remediation, in: Thermodynamics, Solubility and Environmental Issues. pp. 327–340.
Mayer, B.K., Baker, L.A., Boyer, T.H., Drechsel, P., Gifford, M., Hanjra, M.A., Parameswaran, P., Stoltzfus, J., Westerhoff, P., Rittmann, B.E., 2016. Total Value of Phosphorus Recovery. Environ. Sci. Technol. 50, 6606–6620. doi:10.1021/acs.est.6b01239
Murphy, J., Riley, J.P., 1962. A modified single solution method for the determination of phosphate in natural waters. Anal. Chim. Acta 27, 31–36. doi:10.1016/S0003-2670(00)88444-5
Niu, Y., Tan, H., Hui, S., 2016. Ash-related issues during biomass combustion: Alkali-induced slagging, silicate melt-induced slagging (ash fusion), agglomeration, corrosion, ash utilization, and related countermeasures. Prog. Energy Combust. Sci. 52, 1–61. doi:10.1016/j.pecs.2015.09.003
Olsen, S.R., Cole, C. V, Watandbe, F., Dean, L., 1954. Estimation of Available Phosphorus in Soil by Extraction with sodium Bicarbonate. U.S. Dep. Agric. 939.
Olson, B.M., Bremer, E., McKenzie, R.H., Bennett, R., 2010. Phosphorus

accumulation and leaching in two irrigated soils with incremental rates of cattle manure. Can. J. Soil Sci. 90, 355–362. doi:10.4141/CJSS09025
Oshita, K., Sun, X., Kawaguchi, K., Shiota, K., Takaoka, M., Matsukawa, K., Fujiwara, T., 2016. Aqueous leaching of cattle manure incineration ash to produce a phosphate enriched fertilizer. J. Mater. Cycles Waste Manag. 18, 608–617. doi:10.1007/s10163-016-0528-6
Oxmann, J. F., 2014. Technical Note: An X-ray absorption method for the identification of calcium phosphate species using peak-height ratios. Biogeosciences 11(8): 2169-2183.
Parhi, P., Ramanan, A., Ray, A.R., 2006. Hydrothermal Synthesis of nanocrystalline powders of alkaline-earth hydroxyapatites, A10(PO4)6(OH)2 (A = Ca, Sr and Ba). J. Mater. Sci. 41, 1455–1458. doi:10.1007/s10853-006-7460-4
Pettersson, A., Åmand, L.-E., Steenari, B.-M., 2008a. Leaching of ashes from co-combustion of sewage sludge and wood—Part II: The mobility of metals during phosphorus extraction. Biomass Bioenerg. 32, 236–244. doi:10.1016/j.biombioe.2007.09.006
Pettersson, A., Åmand, L.-E., Steenari, B.-M., 2008b. Leaching of ashes from co-combustion of sewage sludge and wood—Part I: Recovery of phosphorus. Biomass Bioenerg. 32, 224–235. doi:10.1016/j.biombioe.2007.09.016
Peters, F., Schwarz K., Epple M., 2000. The structure of bone studied with synchrotron X-ray diffraction, X-ray absorption spectroscopy and thermal analysis. Thermochim. Acta 361(1-2): 131-138.
Petzet, S., Peplinski, B., Cornel, P., 2012. On wet chemical phosphorus recovery from sewage sludge ash by acidic or alkaline leaching and an optimized combination of both. Water Res. 46, 3769–3780. doi:10.1016/j.watres.2012.03.068
Ragauskas, A.J., 2006. The Path Forward for Biofuels and Biomaterials. Science. 311, 484–489. doi:10.1126/science.1114736
Rajendran, J., Gialanella S., Aswath P. B., 2013. XANES analysis of dried and calcined bones. Mat. Sci. Eng. C-Mater. 33(7): 3968-3979.
Ravel, B., Newville M., 2005. ATHENA, ARTEMIS, HEPHAESTUS: data analysis for X-ray absorption spectroscopy using IFEFFIT. J. Synchrotron Radiat. 12: 537-541.
Rittmann, B.E., Mayer, B., Westerhoff, P., Edwards, M., 2011. Capturing the lost phosphorus. Chemosphere 84, 846–853. doi:10.1016/j.chemosphere.2011.02.001
Saidur, R., Abdelaziz, E.A., Demirbas, A., Hossain, M.S., Mekhilef, S., 2011. A review on biomass as a fuel for boilers. Renew. Sustain. Energy Rev. 15, 2262–2289. doi:10.1016/j.rser.2011.02.015
Sattari, S.Z., Bouwman, A.F., Giller, K.E., van Ittersum, M.K., 2012. Residual soil phosphorus as the missing piece in the global phosphorus crisis puzzle. Proc. Natl. Acad. Sci. U. S. A. 109, 6348–53. doi:10.1073/pnas.1113675109
Simons, A., Solomon, D., Chibssa, W., Blalock, G., Lehmann, J., 2014. Filling the phosphorus fertilizer gap in developing countries. Nat. Geosci. 7, 3–3. doi:10.1038/ngeo2049
Stegemann, J.A., Côté, P.L., 1991. Acid Neutralization Capacity, Appendix B: Investigation of test methods for solidified waste evaluation—a cooperative program, Manuscript Series TS-15, Environment Canada Wastewater Technology Centre, Burlington, Ontario Canada.
Štulajterová, R., Medvecký, Ľ., 2008. Effect of calcium ions on transformation brushite to hydroxyapatite in aqueous solutions. Colloids Surfaces A Physicochem. Eng. Asp. 316, 104–109. doi:10.1016/j.colsurfa.2007.08.036

692 Sugiyama, S., Kitora, R., Kinoshita, H., Nakagawa, K., Katoh, M., Nakasaki, K.,
693 2016. Recovery of Calcium Phosphates from Composted Chicken Manure. J.
694 Chem. Eng. Japan 49, 224–228. doi:10.1252/jcej.15we111
695 Szögi, A.A., Vanotti, M.B., Hunt, P.G., 2015. Phosphorus recovery from pig manure
696 solids prior to land application. J. Environ. Manage. 157, 1–7.
697 Tan, Z., Lagerkvist, A., 2011. Phosphorus recovery from the biomass ash: A review.
698 Renew. Sustain. Energy Rev. 15, 3588–3602. doi:10.1016/j.rser.2011.05.016
699 Tayibi, H., Choura, M., López, F.A., Alguacil, F.J., López-Delgado, A., 2009.
700 Environmental impact and management of phosphogypsum. J. Environ. Manage.
701 90, 2377–2386. doi:10.1016/j.jenvman.2009.03.007
702 Tilman, D., Fargione, J., Wolff, B., D'Antonio, C., Dobson, A., Howarth, R.,
703 Schindler, D., Schlesinger, W.H., Simberloff, D., Swackhamer, D., 2001.
704 Forecasting agriculturally driven global environmental change. Science 292,
705 281–284. doi:10.1126/science.1057544
706 Tilman, D., Lehman, C., 1987. Human-caused environmental change : Impacts on
707 plant diversity and evolution. Proc. Natl. Acad. Sci. U. S. A. 98, 5433–5440.
708 doi:10.1073/pnas.091093198
709 Vassilev, S. V., Baxter, D., Andersen, L.K., Vassileva, C.G., 2013a. An overview of
710 the composition and application of biomass ash. Part 2. Potential utilisation,
711 technological and ecological advantages and challenges Fuel 105, 19–39.
712 doi:10.1016/j.fuel.2012.10.001
713 Vassilev, S. V., Baxter, D., Andersen, L.K., Vassileva, C.G., 2013b. An overview of
714 the composition and application of biomass ash. Part 1. Phase–mineral and
715 chemical composition and classification. Fuel 105, 40–76.
716 doi:10.1016/j.fuel.2012.09.041
717 Vassilev, S. V., Baxter, D., Andersen, L.K., Vassileva, C.G., Morgan, T.J., 2012. An
718 overview of the organic and inorganic phase composition of biomass. Fuel 94, 1–
719 33. doi:10.1016/j.fuel.2011.09.030
720 Vassilev, S. V., Baxter, D., Vassileva, C.G., 2013c. An overview of the behaviour of
721 biomass during combustion: Part I. Phase-mineral transformations of organic and
722 inorganic matter. Fuel 112, 391–449. doi:10.1016/j.fuel.2013.05.043
723 Wilfert, P., Kumar, P.S., Korving, L., Witkamp, G.J., Van Loosdrecht, M.C.M., 2015.
724 The Relevance of Phosphorus and Iron Chemistry to the Recovery of Phosphorus
725 from Wastewater: A Review. Environ. Sci. Technol. 49, 9400–9414.
726 doi:10.1021/acs.est.5b00150
727 Williams, A.G., Leinonen, I., Kyriazakis, I., 2016. Environmental benefits of using
728 turkey litter as a fuel instead of a fertiliser. J. Clean. Prod. 113, 167–175.
729 doi:10.1016/j.jclepro.2015.11.044
730 Wu, S., Wang, L., Zhao, L., Zhang, P., El-shall, H., 2018. Recovery of rare earth
731 elements from phosphate rock by hydrometallurgical processes – A critical
732 review. Chem. Eng. J. 335, 774–800. doi:10.1016/j.cej.2017.10.143
733 Zhang, F.S., Yamasaki, S., Kimura, K., 2002. Waste ashes for use in agricultural
734 production: II. Contents of minor and trace metals. Sci. Total Environ. 286, 111–
735 118. doi:10.1016/S0048-9697(01)00968-8
736
737

Figure captions

Fig. 1 X-ray powder diffraction (XRD) (a), Fourier transform infrared spectra (FTIR, normalised) (b), Thermogravimetric (TG/DTG) (c), and P K-edge X-ray absorption near edge structure (XANES, normalised) (d) analyses of meat and bone meal (MBM) bottom ashes (BA) and air pollution control residue (APCr), and poultry litter co-combustion (PL) bottom ash and residues from leaching of the same residues at pH 5.1-6.8. The reference materials Morrocan apatite (carbonate apatite), brushite, and apatite (hydroxyapatite) were all analyzed by FTIR, TG/DTG, and XANES, but only the references most relevant to each figure were presented; XRD references were from the XRD pattern database (International Centre for Diffraction Data, ICDD).

Fig. 2 Concentration of available P in meat and bone meal (MBM) bottom ashes (BA) and air pollution control residue (APCr), and poultry litter co-combustion (PL) bottom ash and residues from leaching of the same residues at pH 5.1-6.8. Error bars represent standard deviation of three replicates.

Fig. 3 Anion leaching from meat and bone meal (MBM) bottom ashes (BA) and air pollution control residue (APCr), and poultry litter co-combustion (PL) bottom ash in the Acid Neutralization Capacity test (circled points are those for which the leached residue was characterised).

Fig. 4 Major element leaching from meat and bone meal (MBM) bottom ashes (BA) and air pollution control residue (APCr), and poultry litter co-combustion (PL) bottom ash in the Acid Neutralization Capacity test (circled points are those for which the leached residue was characterised).

Fig. 5 P recovery (average of duplicates) from meat and bone meal (MBM) bottom ashes (BA) and air pollution control residue (APCr), and poultry litter co-combustion (PL) bottom ash using H_2SO_4 and HNO_3, (a) Acid consumption comparison between H_2SO_4 and HNO_3; (b) P recovery percentage using H_2SO_4. Leaching time 2 h; Solid/liquid ratio 0.1.

Table 1 Acid demand for P recovery

Item	Original TP ($g\ kg^{-1}$)	TP recovery rate (%)	Acid demand (mol H^+/ mol P)	Method and optimal conditions	Comments	Ref.
Swine manure	~16	94% leached to solution	3.78	Hydrothermal acid leaching (S/L: 24 g/220 mL): 170 ℃, 0.1 M H_2SO_4 (pH → 3.5)	Additional thermal consumption.	(Ekpo et al., 2016)
Composited chicken manure	-	-	9.10	Acid leaching (S/L: 1 g/100 mL): 0.1 M HNO_3	Too much wastewater.	(Sugiyama et al., 2016)
Fresh pig manure	4.2	87% leached to solution	6.36	Acid leaching (S/L: 2 g/50 mL): 10 mM citric (pH 6.9 → 3.2)	Extracted residues are safer for land application with a more balanced N: P ratio. Too much wastewater.	(Szögi et al., 2015)
	4.0	88% leached to solution	8.81	Acid leaching (S/L: 2 g/50 mL): 40 mM HCl (pH 7.0 → 1.8)		
Poultry manure hydrochar	32.9	89.7% leached to solution	92.2	Acid leaching (S/L: 10 g/220 mL): 4 M HCl	High acid load. Too much wastewater.	(Heilmann et al., 2014)
Swine manure hydrochar	39.1	89.3% leached to solution	78.1			
Cow manure hydrochar	18.6	98.4% leached to solution	149.1			
Pig manure pyrolysis char	41.2-54.6	~ 90% leached to solution	126.2-167.2	Acid leaching (S/L: 2 g/1000 mL): 0.2 M H_2SO_4	High acid load. Too much wastewater.	(Azuara et al., 2013)
Gasified piggery waste ash	-	94% leached to solution	6.61	Acid leaching: (S/L: 1 g/12.5 mL): 0.8 M H_2SO_4	Higher H_2SO_4 concentration did not improve P dissolution.	(Kuligowski and Poulsen, 2010)
Animal carcasses incineration ash	138.4	57% leached to solution	3.10	Acid leaching: H_2SO_4 (pH 2.0)	Feasible practice	(Cohen, 2009)
		73% leached to solution	3.29	Acid leaching: H_2SO_4 (pH 1.5)		
MBM ashes/PL ashes	84.6-139	About 90% leached to solution	3.1-5.3	Acid leaching: H_2SO_4 or HNO_3 (S/L: 1 g/10 mL, pH around 1.0-1.5)	Feasible practice	This study

Table 2 Elemental analyses of UK biomass bottom ashes (BA) and air pollution control residue (APCr) determined by digestion and ICP-OES, including also total P by colorimetry (*)

Element	MBM1-BA	MBM2-BA	MBM2-APCr	PL1-BA	PL2-BA
Major element (mg/g)					
Al	3.70	1.78	1.58	6.07	3.58
Ca	316	245	246	175	161
Fe	15.3	4.04	2.51	7.34	5.99
K	7.97	50.9	27.0	88.5	119
Mg	7.66	7.23	6.13	37.0	45.2
Mn	0.23	0.18	0.08	3.14	4.09
Na	22.5	88.0	72.7	18.3	21.7
P	131	95.4	97.9	82.8	109
TP*	139	96.3	98.8	84.6	111
Minor element (mg/kg)					
B	113	37.6	23.0	146.8	186
Ba	156	99.0	92.0	228	156
Bi	1.4	0.4	1.2	ND	ND
Cd	ND	ND	ND	ND	ND
Cr	16.7	34.4	26.2	48.8	35.2
Co	10.5	8.6	0.9	6.5	16.1
Cu	183	141	67.8	806	640
Li	ND	ND	ND	1.4	ND
Ni	6.6	7.4	5.5	35.1	22.4
Pb	4.7	41.2	22.8	48.8	2.7
Sr	191	125	130	198	211
Zn	157	830	529	1110	760

ND indicates not detected

Table 3 Mineral phases identified in meat and bone meal (MBM) bottom ashes (BA) and air pollution control residue (APCr), and poultry litter co-combustion (PL) bottom ash and residues from leaching of the same residues at pH 5.1-6.8

Sample	Mineral phases									
	Hydroxyapatite, $Ca_5(PO_4)_3(OH)$	Arcanite, K_2SO_4	Brushite, $CaHPO_4{\cdot}2H_2O$	Calcite, $CaCO_3$	Calcium Sulfate, $CaSO_4$	Gypsum, $CaSO_4{\cdot}2H_2O$	Halite, NaCl	Portlandite, $Ca(OH)_2$	Potassium sodium calcium phosphate, $KNaCa_2(PO_4)_2$	Quartz, SiO_2
MBM1-BA	+			+	+			+		+
MBM1-BA residue (pH 6.2)	+		+			+				+
MBM2-BA	+	+		+	+		+	+		+
MBM2-BA residue (pH 5.1)	+		+			+				+
MBM2-APCr	+	+		+	+		+	+		
MBM2-APCr residue (pH 5.9)	+		+			+				
PL1-BA		+			+				+	+
PL1-BA residue (pH 6.5)			+			+				+
PL2-BA		+			+				+	+
PL2-BA residue (pH 6.8)			+			+				+

Figure

Click here to download Figure: Leng et al 2018-biomass ashes & P recovery (revised)-Figs.docx

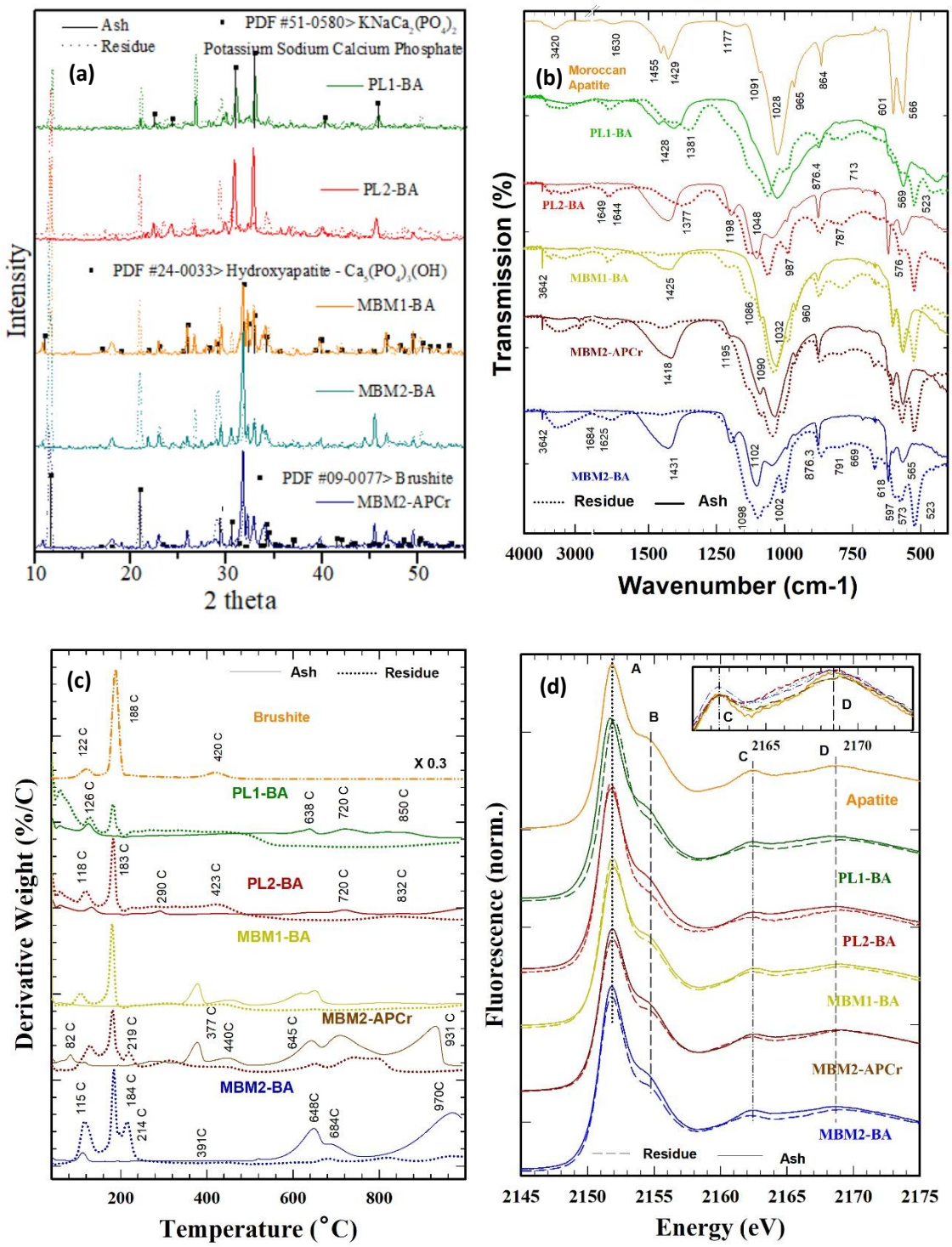

Fig. 1 X-ray powder diffraction (XRD) (a), Fourier transform infrared spectra (FTIR, normalised) (b), Thermogravimetric (TG/DTG) (c), and P K-edge X-ray absorption near edge structure (XANES, normalised) (d) analyses of meat and bone meal (MBM) bottom ashes (BA) and air pollution control residue (APCr), and poultry litter co-combustion (PL) bottom ash and residues from leaching of the same residues at pH 5.1-6.8. The reference materials Morrocan apatite (carbonate apatite), brushite, and apatite (hydroxyapatite) were all analyzed by FTIR, TG/DTG, and XANES, but only the references most relevant to each figure were presented; XRD references were from the XRD pattern database (International Centre for Diffraction Data, ICDD).

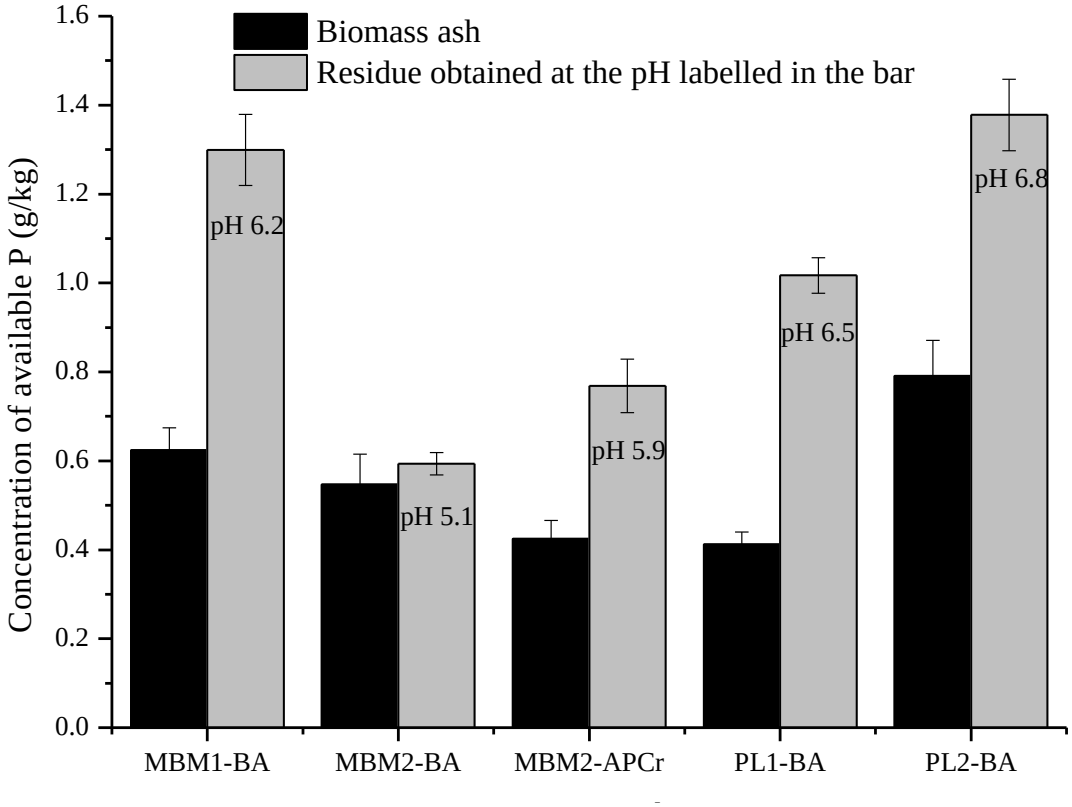

Fig. 2 Concentration of available P in meat and bone meal (MBM) bottom ashes (BA) and air pollution control residue (APCr), and poultry litter co-combustion (PL) bottom ash and residues from leaching of the same residues at pH 5.1-6.8. Error bars represent the standard deviation of three replicates.

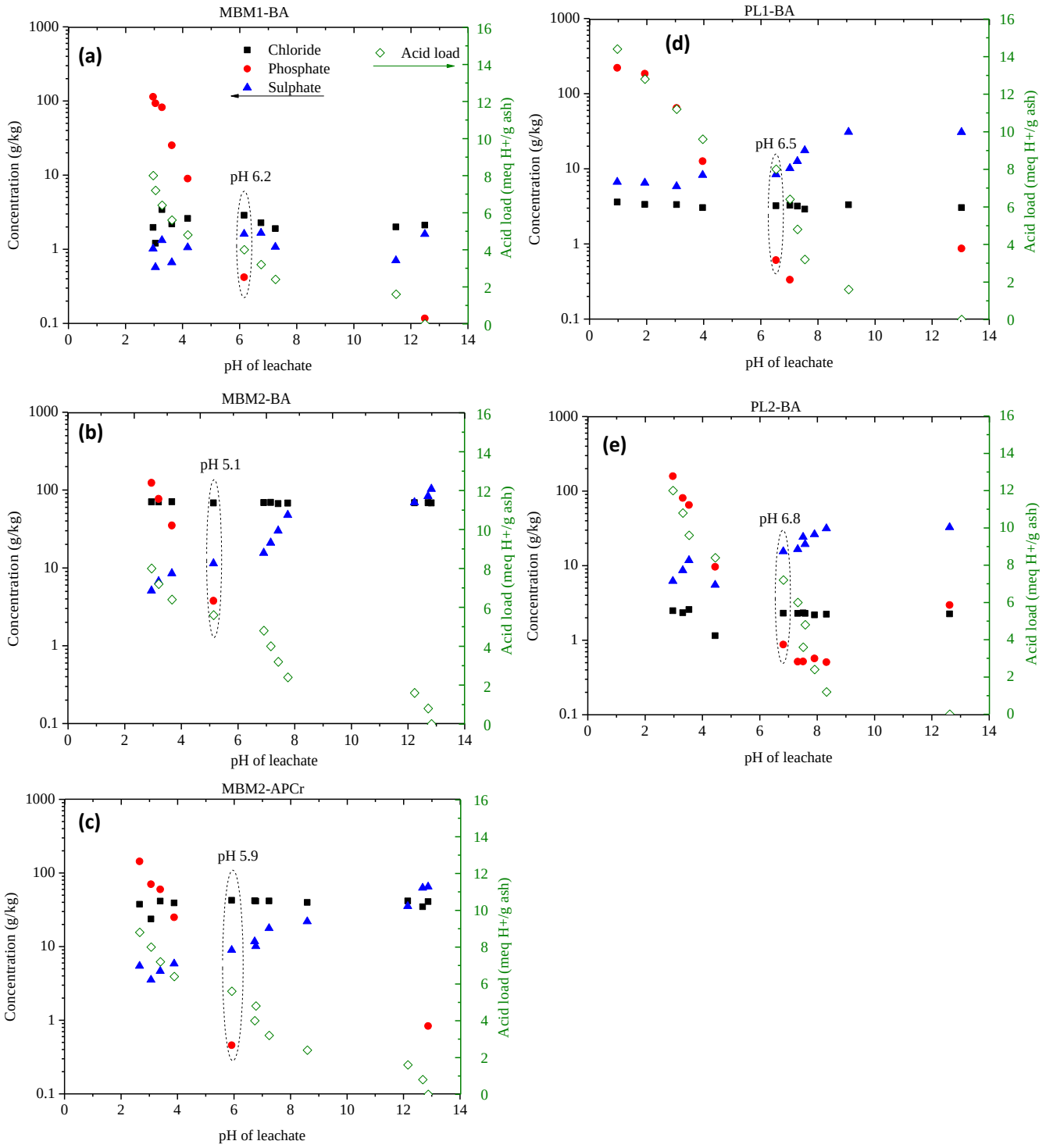

Fig. 3 Anion leaching from meat and bone meal (MBM) bottom ashes (BA) and air pollution control residue (APCr), and poultry litter co-combustion (PL) bottom ash in the Acid Neutralization Capacity test (circled points are those for which the leached residue was characterised).

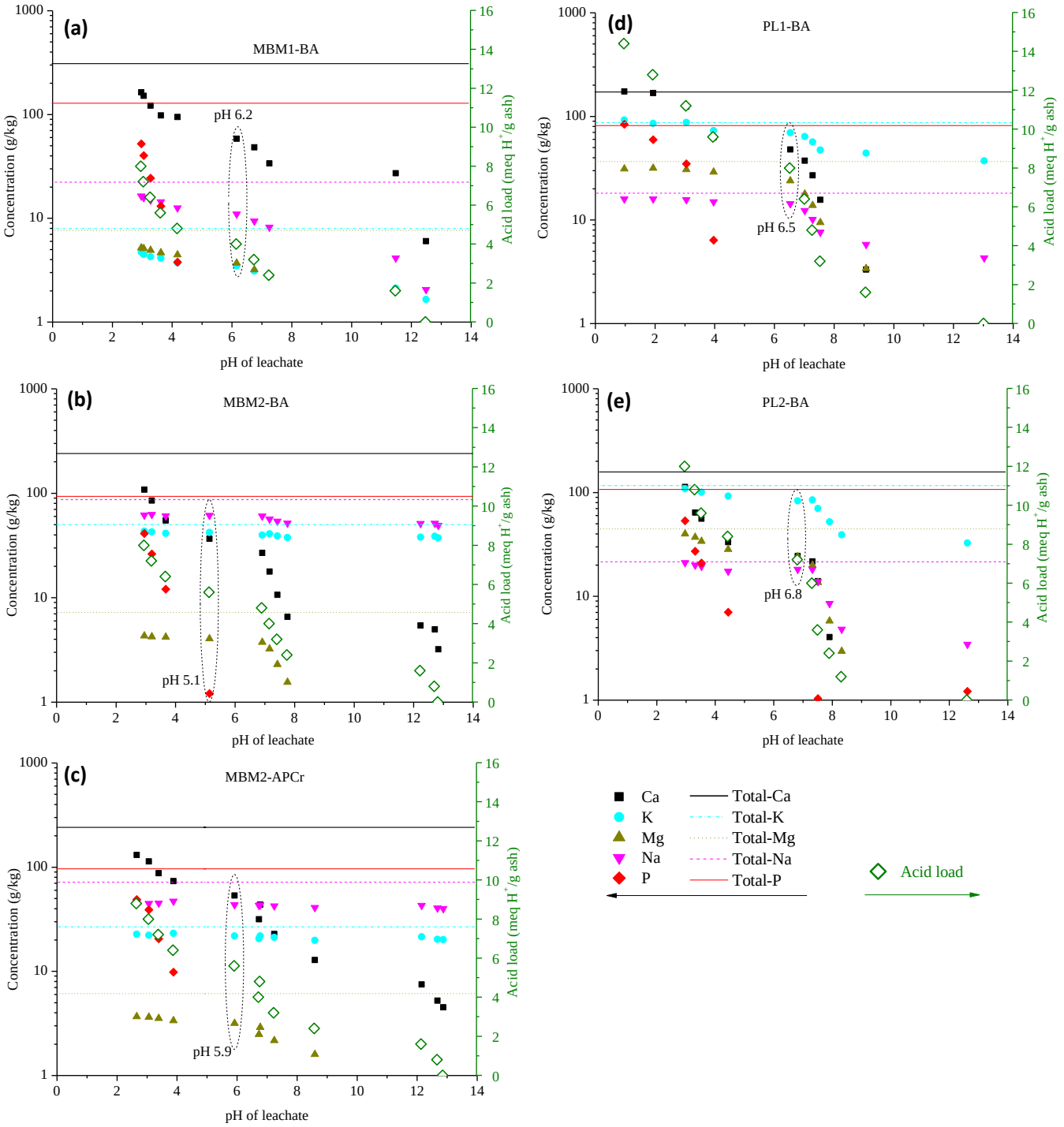

Fig. 4 Major element leaching from meat and bone meal (MBM) bottom ashes (BA) and air pollution control residue (APCr), and poultry litter co-combustion (PL) bottom ash in the Acid Neutralization Capacity test (circled points are those for which the leached residue was characterised).

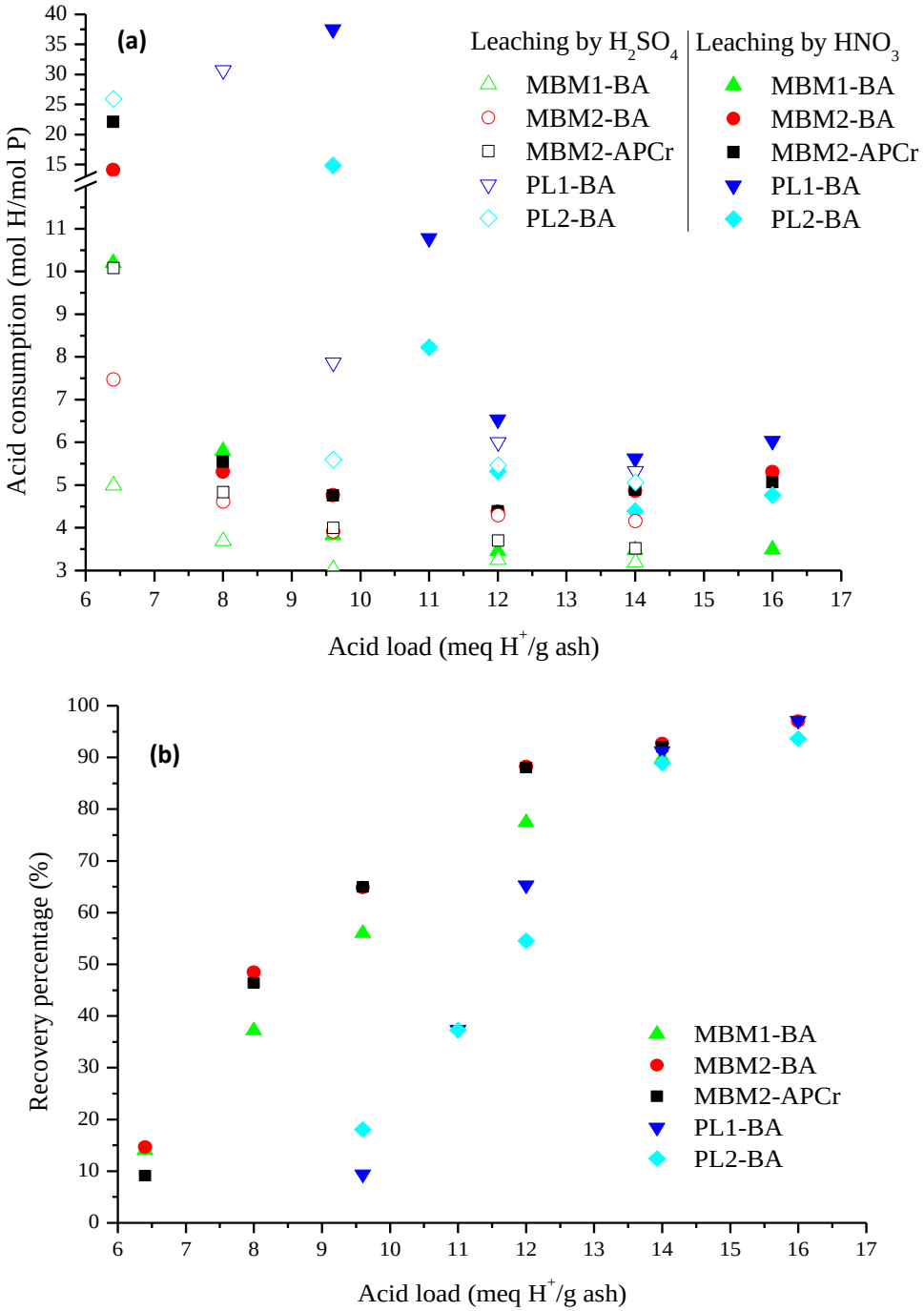

Fig. 5 P recovery (average of duplicates) from meat and bone meal (MBM) bottom ashes (BA) and air pollution control residue (APCr), and poultry litter co-combustion (PL) bottom ash using H_2SO_4 and HNO_3, (a) Acid consumption comparison between H_2SO_4 and HNO_3; (b) P recovery percentage using H_2SO_4. Leaching time 2 h; Solid/liquid ratio 0.1.

Supplementary material for on-line publication only

Click here to download Supplementary material for on-line publication only: Leng et al 2018-biomass ashes & P recovery-SI.doc